International Journal of Solids and Structures, Volume 44, Issues 22–23, November 2007, Pages 7543-7563

Accepted Manuscript

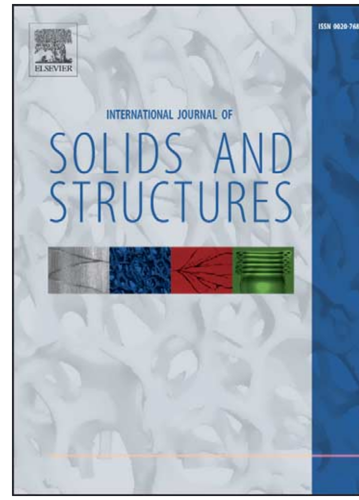

Free vibration of a three-layered sandwich beam using the dynamic stiffness method and experiment

J.R. Banerjee, C.W. Cheung, R. Morishima, M. Perera, J. Njuguna

PII: S0020-7683(07)00206-5
DOI: 10.1016/j.ijsolstr.2007.04.024
Reference: SAS 5949

To appear in: *International Journal of Solids and Structures*

Received Date: 15 January 2007
Revised Date: 15 April 2007
Accepted Date: 24 April 2007

Please cite this article as: Banerjee, J.R., Cheung, C.W., Morishima, R., Perera, M., Njuguna, J., Free vibration of a three-layered sandwich beam using the dynamic stiffness method and experiment, *International Journal of Solids and Structures* (2007), doi: 10.1016/j.ijsolstr.2007.04.024

Free vibration of a three-layered sandwich beam using the dynamic stiffness method and experiment

J.R. Banerjee,* C.W. Cheung, R. Morishima, and M. Perera

School of Engineering and Mathematical Sciences, City University, London EC1V OHB, UK

J. Njuguna

School of Industrial and Manufacturing Science, Cranfield University, Cranfield,

Bedfordshire MK43 0AL, UK

Abstract

In this paper an accurate dynamic stiffness model for a three-layered sandwich beam of unequal thicknesses is developed and subsequently used to investigate its free vibration characteristics. Each layer of the beam is idealised by the Timoshenko beam theory and the combined system is reduced to a tenth order system using symbolic computation. An exact dynamic stiffness matrix is then developed by relating amplitudes of harmonically varying loads to those of the responses. The resulting dynamic stiffness matrix is used with particular reference to the Wittrick-Williams algorithm to carry out the free vibration analysis of a few illustrative examples. The accuracy of the theory is confirmed both by published literature and by experiment. The paper closes with some concluding remarks.

Keywords: Dynamic stiffness method; Free vibration; Sandwich beam; Timoshenko theory, Wittrick–Williams algorithm; Symbolic computation

*Corresponding author, Tel: +44 (0)2070408924, fax: +44(0)2070408566

1. Introduction

The dynamic behaviour of sandwich beams is well researched and the literature has been around for nearly half a century. A sample of selected papers published in recent years is given in the list of references, which review the state of the art and provide numerous cross-references on the subject. One of the main reasons for conducting research in this area is due to the fact that sandwich constructions offer designers a number of advantages of which, perhaps the most important one is the high strength to weight ratio. This can be crucial, particularly in aerospace design, where weight saving is, as always, a major consideration. The published literature on the free vibration analysis of sandwich beams deals mainly with three layered sandwich beams that are elastic (and some times viscoelastic), homogeneous and isotropic, but rigidly joined together, and for which the top and bottom layers are generally made of strong materials such as steel or aluminium whereas the core (i.e. the middle layer) is relatively soft, for example, rubber or honeycomb structures, so as to provide adequate damping and good energy absorption characteristics. A majority of the analyses reported, appear to have been carried out either by using the solution of the classical governing differential equations and thereby imposing the boundary conditions or by using the conventional finite element methods. However, in recent years, Banerjee (2003), Banerjee and Sobey (2005), and Howson and Zare (2005) used a different approach, which is that of the dynamic stiffness method. The authors of these papers have pointed out that there are many advantages of the dynamic stiffness method in that it is probably the most accurate method (often called an exact method) and unlike the finite element and other approximate methods, the model accuracy is not unduly compromised, as a result of using a small number of elements in the analysis. For instance, one single structural element can be used in the dynamic stiffness method to compute any number of natural frequencies to any desired accuracy. This is, of course, impossible in the finite element and other approximate methods. Earlier investigators of the free vibration analysis of sandwich beams using the dynamics stiffness method have had varying degrees of success. However, it is to be noted that during the developments of the dynamic stiffness method, especially for solving the sandwich beam vibration problem, there were considerable difficulties due to lack of knowledge and scarcity of literature on the subject. Thus, in the initial stages, simplifying assumptions were made and the choice of the allowable displacement was significantly restricted. This was probably justified at the time, particularly in view of the complexities involved in deriving as well as solving the governing differential equations in closed analytical form that are basic requirements in the dynamic stiffness method. For instance, Banerjee (2003) in his earlier work assumed that the top and bottom layers of the sandwich beam behave according to the Bernoulli-Euler beam theory whereas the core deforms only in shear. This was no-doubt restrictive, but nevertheless, the theory worked well for certain classes of problems, particularly in the lower frequency range. A couple of years later, Banerjee and Sobey (2005) improved the model substantially, by idealising the top and bottom layers as Rayleigh beams whereas the central core as a Timoshenko beam. This recent development which led to an eight-order system as opposed to the sixth order one in the former, benefited very considerably from the use of symbolic computation when manipulating the algebra. Without the application of symbolic computation the work would have been very difficult, and probably impossible. With the advent of symbolic computation, the research using the dynamic stiffness method to solve free vibration problems has no-doubt been facilitated, which partly motivated this work.

The current study advances the earlier studies of Banerjee (2003) and Banerjee and Sobey (2005) significantly, by modelling each layer of the sandwich beam as a Timoshenko beam. This resulted in a tenth order system as opposed to the sixth (Banerjee, 2003) and eight (Banerjee and Sobey, 2005) order systems in previous studies. As it will be shown later, the derivation of the governing differential equations of motion of the system, development of the dynamic stiffness matrix and finally application of the dynamic stiffness matrix to solve the free vibration problem are of considerable complexity, requiring substantial amount of symbolic and numerical computations. The investigation is carried out in following steps : (i) first the energy expressions of a three-layered asymmetric sandwich beam are formulated using the theory of elasticity, (ii) secondly, Hamilton's principle is applied to derive the governing differential equations of motion and associated natural boundary conditions, (iii) next, by assuming harmonic oscillation, the differential equations are combined into a tenth order system by making extensive use of symbolic computation, (iv) the tenth order system is then solved in closed analytical form, (v) subsequently, the frequency dependent dynamic stiffness matrix of the system is derived by relating the amplitudes of the axial forces, shear forces and bending moments to those of the axial and flexural displacements and bending rotations, (vi) the well known algorithm of Wittrick and Williams (1971) is then applied to the resulting dynamic stiffness matrix for free vibration analysis of some illustrative examples, and (vi) finally, the theory is validated by experiment using an impulse hammer kit.

2. Theory

2.1 Derivation of the governing differential equations of motion in free vibration and solution

The following general assumptions are made when developing the governing differential equations of motion in free vibration of a three layered sandwich beam of asymmetric cross-section.

(i) All displacements and strains are small so that the theory of linear elasticity applies.

(ii) The faces and core of the sandwich beam are made of homogeneous and isotropic materials and the variation of strain within them is linear.

(iii) Transverse normal strains in the faces and core are negligible.

(iv) There is no slippage or delamination between the layers during deformation.

In a rectangular Cartesian coordinate system, Fig. 1 shows a three-layered sandwich beam of length L. Each layer has its own geometric and material properties with a subscript i denoting the layer number (i=1 for the top layer). Thus each layer has thickness h_i, width b_i (so that area $A_i = b_i h_i$), second moment of area I_i, density ρ_i, (so that the mass per unit length $m_i = \rho_i A_i$), Young's modulus E_i, shear modulus G_i, and shear correction or shape factor k_i (k_i <1).

The system of displacements used is as follows. All three layers have a common flexure in the *y*-direction with the flexural displacement denoted by *w*. The axial displacement (i.e. the displacement in the *x*-direction) of the mid-plane of each layer is u_i (i = 1, 2 and 3) which varies linearly through the thickness. The axial displacement of the interface between layers 1 and 2 is u_{12} whereas for that of the interface between layers 2 and 3 is u_{23} as shown in Fig. 1. The cross-section of each layer does not rotate so as to be normal to the common flexure, but it necessarily shears leading to the Timoshenko beam formulation.

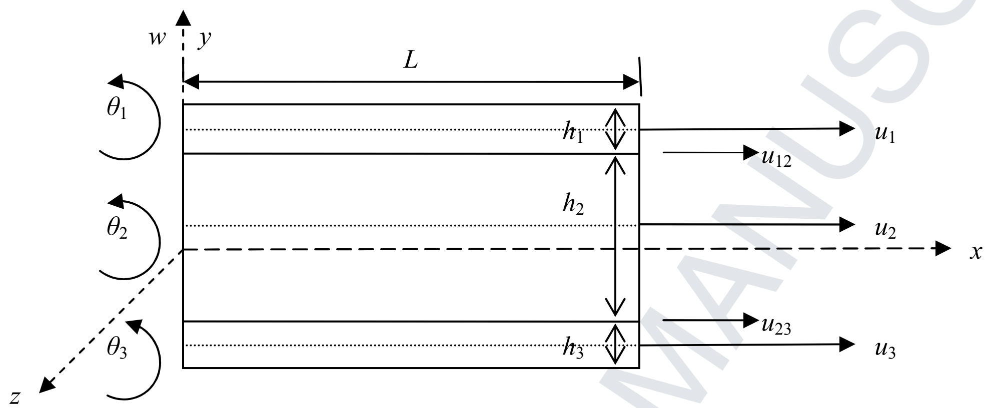

Fig. 1. The coordinate system and notation for a three-layered sandwich beam

Given the displacement system in layers 1 and 3, the displacement in layer 2 is fully determinate. This carries over into axial stress, which is dependent on derivatives with respect to *x* of u_i and velocity with time derivatives. Thus a model can be developed in which the behaviour of the central layer is described in terms of the behaviour of the outer layers.

Using the continuity of deformation, the displacement u_{12} and u_{23} at the layer boundaries can be expressed as

$$u_{12} = u_1 + (h_1/2)\theta_1 = u_2 - (h_2/2)\theta_2 \tag{1}$$

$$u_{23} = u_3 - (h_3/2)\theta_3 = u_2 + (h_2/2)\theta_2 \tag{2}$$

Equations (1) and (2) give

$$2u_2 = u_1 + u_3 + \left(h_1\theta_1 - h_3\theta_3\right)/2 \tag{3}$$

$$h_2\theta_2 = u_3 - u_1 - \left(h_1\theta_1 + h_3\theta_3\right)/2 \tag{4}$$

By allowing each of the three layers to have the same flexural displacement *w* in direction *oy*, the local rotations $\theta_1, \theta_2, \theta_3$ which are not identified with w', where the prime denotes differentiation with respect to *x*, a Timoshenko beam type model can be constructed. Each layer has linear variation of axial displacement and stress with respect to *y* in the cross-section, but the shear stress and strain remain constant.

In developing the strain and kinetic energies, repeated use is made of the following well-known results.

If $f(x)$ is a linear function of x varying from $f_1 = f(x_1)$ at $x = x_1$ to $f_2 = f(x_2)$ at $x = x_2$ then

$$\int_{x_1}^{x_2} [f(x)]^2\, dx = (x_2 - x_1)(f_1^2 + f_1 f_2 + f_2^2)/3 \tag{5}$$

Strain energy due to axial stress in layer 1 is given by

$$U_{B_1} = \frac{1}{2}\int\int\int_V E_1[\varepsilon_x]^2\, dxdydz \tag{6}$$

where ε_x varies linearly from $u_1' - \frac{h_1}{2}\theta_1'$ to $u_1' + \frac{h_1}{2}\theta_1'$ through the thickness

Noting that the width b_1 of layer 1 is constant, the strain energy U_{B_1} becomes

$$
\left.\begin{aligned}
U_{B1} &= \frac{1}{2}\int_0^L E_1 \frac{b_1 h_1}{3}\left[\left(u_1' - \frac{h_1}{2}\theta_1'\right)^2 + \left(u_1' - \frac{h_1}{2}\theta_1'\right)\left(u_1' + \frac{h_1}{2}\theta_1'\right) + \left(u_1' + \frac{h_1}{2}\theta_1'\right)^2\right]dx \\
&= \frac{1}{2}\int_0^L E_1 \frac{b_1 h_1}{3}\left[(u_1')^2 - u_1' h_1 \theta_1' + \frac{h_1^2}{4}(\theta_1')^2 + (u_1')^2 - \left(\frac{h_1}{2}\right)^2(\theta_1')^2 + (u_1')^2 + u_1' h_1 \theta_1' + \left(\frac{h_1}{2}\right)^2(\theta_1')^2\right]dx \\
&= \frac{1}{2}\int_0^L E_1 b_1\left[h_1 (u_1')^2 + \frac{h_1^3}{12}(\theta_1')^2\right]dx \\
&= \frac{1}{2}\int_0^L \left[E_1 A_1 (u_1')^2 + E_1 I_1 (\theta_1')^2\right]dx
\end{aligned}\right\} \qquad (7)
$$

where $I_1 = \frac{b_1 h_1^3}{12}$ is the second moment of area of the cross-section and E_1A_1 and E_1I_1 are respectively extensional (or axial) and bending (or flexural) rigidities of layer 1

It follows that total strain energy due to axial stresses in all three layers is

$$
U_B = \frac{1}{2}\int_0^L \left\{E_1 A_1 (u_1')^2 + E_2 A_2 (u_2')^2 + E_3 A_3 (u_3')^2 + E_1 I_1 (\theta_1')^2 + E_2 I_2 (\theta_2')^2 + E_3 I_3 (\theta_3')^2\right\}dx \qquad (8)
$$

In layer 1, the shear strain is $\gamma_1 = w' - \theta_1$ and this is presumed constant across the cross-section. The strain energy due to shear force in layer 1 is given by (Banerjee and Sobey, 2005)

$$
U_{S1} = \frac{1}{2}\int_0^L k_1 A_1 G_1 (w' - \theta_1)^2 \, dx \qquad (9)
$$

where $k_1A_1G_1$ is the shear rigidity of layer 1.

Strain energy due to shear forces in layers 2 and 3 can similarly be obtained and the total strain energy of the whole beam due to shearing is given by

$$
U_S = \frac{1}{2}\int_0^L \left\{k_1 A_1 G_1 (w' - \theta_1)^2 + k_2 A_2 G_2 (w' - \theta_2)^2 + k_3 A_3 G_3 (w' - \theta_3)^2\right\}dx \qquad (10)
$$

Thus the total strain energy U of the sandwich beam due to normal and shear strains can be written as

$$U=\frac{1}{2}\int_0^L\Big[\Big\{E_1A_1(u_1')^2+E_2A_2(u_2')^2+E_3A_3(u_3')^2+E_1I_1(\theta_1')^2+E_2I_2(\theta_2')^2+E_3I_3(\theta_3')^2\Big\} \\ +\Big\{k_1A_1G_1(w'-\theta_1)^2+k_2A_2G_2(w'-\theta_2)^2+k_3A_3G_3(w'-\theta_3)^2\Big\}\Big]dx \tag{11}$$

For the kinetic energy, the axial velocity in layer 1 varies linearly from $\dot{u}_1-\frac{h_1}{2}\dot{\theta}_1$ to $\dot{u}_1+\frac{h_1}{2}\dot{\theta}_1$, so that the kinetic energy T_1 for layer 1 is

$$\left.\begin{aligned} T_1 &= \frac{1}{2}\int_0^L\rho_1 b_1\frac{h_1}{3}\left[\left(\dot{u}_1-\frac{h_1}{2}\dot{\theta}_1\right)^2+\left(\dot{u}_1-\frac{h_1}{2}\dot{\theta}_1\right)\left(\dot{u}_1+\frac{h_1}{2}\dot{\theta}_1\right)+\left(\dot{u}_1+\frac{h_1}{2}\dot{\theta}_1\right)^2\right]dx \\ &=\frac{1}{2}\int_0^L\rho_1 b_1\left[h_1(\dot{u}_1)^2+\frac{h_1^{\,3}}{12}(\dot{\theta}_1)^2\right]dx \\ &=\frac{1}{2}\int_0^L\left[\rho_1A_1(\dot{u}_1)^2+\rho_1I_1(\dot{\theta}_1)^2\right]dx \end{aligned}\right\} \tag{12}$$

In this way the total kinetic energy T of the sandwich beam can be expressed as

$$T=\frac{1}{2}\int_0^L\left\{M\dot{w}^2+\rho_1A_1\dot{u}_1^2+\rho_2A_2\dot{u}_2^{\,2}+\rho_3A_3\dot{u}_3^{\,2}+\rho_1I_1\dot{\theta}_1^2+\rho_2I_2\dot{\theta}_2^2+\rho_3I_3\dot{\theta}_3^2\right\}dx \tag{13}$$

where the first term is the transverse velocity contribution to the kinetic energy, and $M=\rho_1A_1+\rho_2A_2+\rho_3A_3$ represents the mass per unit length of the whole sandwich beam.

The problem can now be processed using Hamilton's Principle, in which δu_2 and $\delta\theta_2$ are expressible in terms of the allowable variations δu_1 , δu_3 , $\delta\theta_1$, $\delta\theta_3$. The displacements u_2 and θ_2 will be substituted from Eqs. (3) and (4) once the variational analysis is complete.

Combining T and U from Eqs. (13) and (11) the Lagrangian $L=T-U$ takes the following form

$$
\left.\begin{aligned}
L=\frac{1}{2}\int_0^L\Big\{&M\dot{w}^2+\rho_1A_1(\dot{u}_1)^2+\rho_2A_2(\dot{u}_2)^2+\rho_3A_3(\dot{u}_3)^2+\rho_1I_1(\dot{\theta}_1)^2+\rho_2I_2(\dot{\theta}_2)^2+\rho_3I_3(\dot{\theta}_3)^2\\
&-E_1A_1(u_1')^2-E_2A_2(u_2')^2-E_3A_3(u_3')^2-E_1I_1(\theta_1')^2-E_2I_2(\theta_2')^2-E_3I_3(\theta_3')^2\\
&-k_1A_1G_1(w'-\theta_1)^2-k_2A_2G_2(w'-\theta_2)^2-k_3A_3G_3(w'-\theta_3)^2\Big\}dx
\end{aligned}\right\} \tag{14}
$$

By applying Hamilton's principle $\delta\int_{t_1}^{t_2}Ldt=0$ and using L from Eq. (14), the following set of differential equations are obtained

$$
\left.\begin{aligned}
&\left[-\left(\rho_1A_1+\frac{1}{3}\rho_2A_2\right)\frac{\partial^2}{\partial t^2}+\left(E_1A_1+\frac{1}{3}E_2A_2\right)\frac{\partial^2}{\partial x^2}-\left(\frac{k_2A_2G_2}{h_2^2}\right)\right]u_1+\left[\left(-\frac{\rho_2A_2}{6}\right)\frac{\partial^2}{\partial t^2}+\left(\frac{E_2A_2}{6}\right)\frac{\partial^2}{\partial x^2}\right.\\
&\left.+\left(\frac{k_2A_2G_2}{h_2^{\,2}}\right)\right]u_3+\left[\left(-\frac{\rho_2A_2}{6}\right)\frac{\partial^2}{\partial t^2}+\left(\frac{E_2A_2}{6}\right)\frac{\partial^2}{\partial x^2}-\left(\frac{k_2A_2G_2}{2h_2^2}\right)\right]h_1\theta_1+\left[\left(\frac{\rho_2A_2}{12}\right)\frac{\partial^2}{\partial t^2}-\left(\frac{E_2A_2}{12}\right)\frac{\partial^2}{\partial x^2}\right.\\
&\left.-\left(\frac{k_2A_2G_2}{2h_2^2}\right)\right]h_3\theta_3-\left(\frac{k_2A_2G_2}{h_2}\right)\frac{\partial w}{\partial x}=0
\end{aligned}\right\} \tag{15}
$$

$$
\left.\begin{aligned}
&\left[\left(-\frac{\rho_2A_2}{6}\right)\frac{\partial^2}{\partial t^2}+\left(\frac{E_2A_2}{6}\right)\frac{\partial^2}{\partial x^2}+\left(\frac{k_2A_2G_2}{h_2^2}\right)\right]u_1+\left[\left(-\frac{\rho_2A_2}{3}-\rho_3A_3\right)\frac{\partial^2}{\partial t^2}+\left(\frac{E_2A_2}{3}+E_3A_3\right)\frac{\partial^2}{\partial x^2}\right.\\
&\left.-\left(\frac{k_2A_2G_2}{h_2^2}\right)\right]u_3+\left[\left(-\frac{\rho_2A_2}{12}\right)\frac{\partial^2}{\partial t^2}+\left(\frac{E_2A_2}{12}\right)\frac{\partial^2}{\partial x^2}+\left(\frac{k_2A_2G_2}{2h_2^2}\right)\right]h_1\theta_1+\left[\left(\frac{\rho_2A_2}{6}\right)\frac{\partial^2}{\partial t^2}-\left(\frac{E_2A_2}{6}\right)\frac{\partial^2}{\partial x^2}\right.\\
&\left.+\left(\frac{k_2A_2G_2}{2h_2^2}\right)\right]h_3\theta_3+\left(\frac{k_2A_2G_2}{h_2}\right)\frac{\partial w}{\partial x}=0
\end{aligned}\right\} \tag{16}
$$

$$
\left.\begin{aligned}
&\left[\left(-\frac{\rho_2A_2}{6}\right)\frac{\partial^2}{\partial t^2}+\left(\frac{E_2A_2}{6}\right)\frac{\partial^2}{\partial x^2}-\left(\frac{k_2A_2G_2}{2h_2^2}\right)\right]h_1u_1+\left[\left(-\frac{\rho_2A_2}{12}\right)\frac{\partial^2}{\partial t^2}+\left(\frac{E_2A_2}{12}\right)\frac{\partial^2}{\partial x^2}+\left(\frac{k_2A_2G_2}{2h_2^2}\right)\right]h_1u_3\\
&+\left[-\left(\rho_1I_1+\frac{h_1^2}{12}\rho_2A_2\right)\frac{\partial^2}{\partial t^2}+\left(E_1I_1+\frac{h_1^2}{12}E_2A_2\right)\frac{\partial^2}{\partial x^2}-\left(k_1A_1G_1+\left(\frac{h_1^2}{4h_2^2}\right)k_2A_2G_2\right)\right]\theta_1\\
&+\left[\left(\frac{\rho_2A_2}{24}\right)\frac{\partial^2}{\partial t^2}-\left(\frac{E_2A_2}{24}\right)\frac{\partial^2}{\partial x^2}-\left(\frac{k_2A_2G_2}{4h_2^2}\right)\right]h_1h_3\theta_3+\left(k_1A_1G_1-\left(\frac{h_1}{2h_2}\right)k_2A_2G_2\right)\frac{\partial w}{\partial x}=0
\end{aligned}\right\} \tag{17}
$$

$$\left[\left(\frac{\rho_2 A_2}{12}\right)\frac{\partial^2}{\partial t^2}-\left(\frac{E_2 A_2}{12}\right)\frac{\partial^2}{\partial x^2}-\left(\frac{k_2 A_2 G_2}{2h_2^2}\right)\right]h_3 u_1+\left[\left(\frac{\rho_2 A_2}{6}\right)\frac{\partial^2}{\partial t^2}-\left(\frac{E_2 A_2}{6}\right)\frac{\partial^2}{\partial x^2}+\left(\frac{k_2 A_2 G_2}{2h_2^2}\right)\right]h_3 u_3$$
$$+\left[\left(\frac{\rho_2 A_2}{24}\right)\frac{\partial^2}{\partial t^2}-\left(\frac{E_2 A_2}{24}\right)\frac{\partial^2}{\partial x^2}-\left(\frac{k_2 A_2 G_2}{4h_2^2}\right)\right]h_1 h_3\theta_1+\left[-\left(\frac{h_3^2}{12}\rho_2 A_2+\rho_3 I_3\right)\frac{\partial^2}{\partial t^2}+\left(E_3 I_3+\frac{h_3^2 E_2 A_2}{12}\right)\frac{\partial^2}{\partial x^2}\right.$$
$$\left.-\left(\frac{h_3^2}{4h_2^2}k_2 A_2 G_2+k_3 A_3 G_3\right)\right]\theta_3-\left(\frac{h_3}{2h_2}k_2 A_2 G_2-k_3 A_3 G_3\right)\frac{\partial w}{\partial x}=0 \qquad (18)$$

$$-\left(\frac{k_2 A_2 G_2}{h_2}\right)\frac{\partial u_1}{\partial x}+\left(\frac{k_2 A_2 G_2}{h_2}\right)\frac{\partial u_3}{\partial x}+\left(k_1 A_1 G_1-\frac{h_1}{2h_2}k_2 A_2 G_2\right)\frac{\partial \theta_1}{\partial x}+\left(-\frac{h_3}{2h_2}k_2 A_2 G_2+k_3 A_3 G_3\right)\frac{\partial \theta_3}{\partial x}$$
$$+\left[-\left(k_1 A_1 G_1+k_2 A_2 G_2+k_3 A_3 G_3\right)\frac{\partial^2}{\partial x^2}+M\frac{\partial^2}{\partial t^2}\right]w=0 \qquad (19)$$

Note the symmetry of the differential operators in Eqs. (15)–(19).

The associated boundary conditions generated by Hamilton's principle are as follows. The axial forces in layers 1 and 3 (F_1 and F_3) are

$$F_1=-\left(E_1 A_1+\frac{E_2 A_2}{4}+\frac{E_2 I_2}{h_2{}^2}\right)\frac{\partial u_1}{\partial x}-\left(\frac{E_2 A_2}{4}-\frac{E_2 I_2}{h_2{}^2}\right)\frac{\partial u_3}{\partial x}-\left(\frac{h_1 E_2 A_2}{8}+\frac{h_1 E_2 I_2}{2h_2{}^2}\right)\frac{\partial \theta_1}{\partial x}-\left(-\frac{h_3 E_2 A_2}{8}+\frac{h_3 E_2 I_2}{2h_2{}^2}\right)\frac{\partial \theta_3}{\partial x} \qquad (20)$$

$$F_3=-\left(\frac{E_2 A_2}{4}-\frac{E_2 I_2}{h_2{}^2}\right)\frac{\partial u_1}{\partial x}-\left(E_3 A_3+\frac{E_2 A_2}{4}+\frac{E_2 I_2}{h_2{}^2}\right)\frac{\partial u_3}{\partial x}-\left(\frac{h_1 E_2 A_2}{8}-\frac{h_1 E_2 I_2}{2h_2{}^2}\right)\frac{\partial \theta_1}{\partial x}-\left(-\frac{h_3 E_2 A_2}{8}-\frac{h_3 E_2 I_2}{2h_2{}^2}\right)\frac{\partial \theta_3}{\partial x} \qquad (21)$$

Note that each of the above two forces includes a contribution from layer 2.

The bending moments in layers 1 and 3 (M_1 and M_3) are

$$M_1=-\left(\frac{h_1 E_2 A_2}{8}+\frac{h_1 E_2 I_2}{2h_2{}^2}\right)\frac{\partial u_1}{\partial x}-\left(\frac{h_1 E_2 A_2}{8}-\frac{h_1 E_2 I_2}{2h_2{}^2}\right)\frac{\partial u_3}{\partial x}-\left(E_1 I_1+\frac{h_1{}^2 E_2 A_2}{16}+\frac{h_1{}^2 E_2 I_2}{4h_2{}^2}\right)\frac{\partial \theta_1}{\partial x}-\left(-\frac{h_1 h_3 E_2 A_2}{16}+\frac{h_1 h_3 E_2 I_2}{4h_2{}^2}\right)\frac{\partial \theta_3}{\partial x} \qquad (22)$$

$$M_3=-\left(-\frac{h_3 E_2 A_2}{8}+\frac{h_3 E_2 I_2}{2h_2{}^2}\right)\frac{\partial u_1}{\partial x}-\left(-\frac{h_3 E_2 A_2}{8}-\frac{h_3 E_2 I_2}{2h_2{}^2}\right)\frac{\partial u_3}{\partial x}-\left(-\frac{h_1 h_3 E_2 A_2}{16}+\frac{h_1 h_3 E_2 I_2}{4h_2{}^2}\right)\frac{\partial \theta_1}{\partial x}-\left(E_3 I_3+\frac{h_3{}^2 E_2 A_2}{16}+\frac{h_3{}^2 E_2 I_2}{4h_2{}^2}\right)\frac{\partial \theta_3}{\partial x} \qquad (23)$$

Note that each of the above two moments includes a contribution from layer 2.

The total shear force, S, in the y direction, is given by

$$S = -\left(k_1 A_1 G_1 + k_2 A_2 G_2 + k_3 A_3 G_3\right)\frac{\partial w}{\partial x} - \left(\frac{k_2 A_2 G_2}{h_2}\right)u_1 + \left(\frac{k_2 A_2 G_2}{h_2}\right)u_3 - \left(-k_1 A_1 G_1 + \frac{h_1 k_2 A_2 G_2}{2h_2}\right)\theta_1 - \left(-k_3 A_3 G_3 + \frac{h_3 k_2 A_2 G_2}{2h_2}\right)\theta_3 \tag{24}$$

Now for harmonic oscillation u_1, u_3, θ_1, θ_3 and w may be written in the following form

$$u_1 = U_1 e^{i\omega t}; \quad u_3 = U_3 e^{i\omega t}; \quad \theta_1 = \Theta_1 e^{i\omega t}; \quad \theta_3 = \Theta_3 e^{i\omega t}; \quad w = W e^{i\omega t} \tag{25}$$

where U_1, U_3, Θ_1, Θ_3 and W, are the amplitudes of u_1, u_3,, θ_1, θ_3 and w, and ω is the angular (or circular) frequency of free vibration, and $i = \sqrt{-1}$

Substituting Eq. (25) into Eqs. (15)-(19) and introducing a non-dimensional length $\xi = x/L$ and writing $D = \frac{d}{d\xi}$ one obtains

$$\left(D^2 + a\right)U_1 + \left(bD^2 + c\right)U_3 + h_1\left(bD^2 + e\right)\Theta_1 - \frac{h_3}{2}\left(bD^2 + c\right)\Theta_3 - \left(fD\right)W = 0 \tag{26}$$

$$\left(bD^2 + c\right)U_1 + \left(gD^2 + h\right)U_3 + \frac{h_1}{2}\left(bD^2 + c\right)\Theta_1 - h_3\left(bD^2 + e\right)\Theta_3 + \left(fD\right)W = 0 \tag{27}$$

$$\left(bD^2 + e\right)U_1 + \frac{1}{2}\left(bD^2 + c\right)U_3 + h_1\left(zD^2 + m\right)\Theta_1 - \frac{h_3}{4}\left(bD^2 + c\right)\Theta_3 + \left(nD\right)W = 0 \tag{28}$$

$$-\frac{1}{2}\left(bD^2 + c\right)U_1 - \left(bD^2 + e\right)U_3 - \frac{h_1}{4}\left(bD^2 + c\right)\Theta_1 + h_3\left(pD^2 + q\right)\Theta_3 - \left(rD\right)W = 0 \tag{29}$$

$$-\left(fD\right)U_1 + \left(fD\right)U_3 + h_1\left(nD\right)\Theta_1 - h_3\left(rD\right)\Theta_3 - \left(sD^2 + t\right)W = 0 \tag{30}$$

where a, b, c, e etc are non-dimensional quantities dependent on the sandwich beam parameters and are defined in Appendix I.

By extensive algebraic manipulation the differential equations (26)-(30) can be combined into a single tenth order differential equation satisfied by U_1, U_3, Θ_1, Θ_3 and W as follows. (This task probably would have been impossible without the use of symbolic computation.)

$$\left(D^{10} + \mu_1 D^8 + \mu_2 D^6 + \mu_3 D^4 + \mu_4 D^2 + \mu_5\right)\Phi = 0 \tag{31}$$

where $\Phi = U_1, \text{or } U_3, \text{or } \Theta_1, \text{or } \Theta_3, \text{or } W$.

The coefficients $\mu_j \, (j = 1, 2, ..., 5)$ are given by

$$\mu_1 = \frac{\eta_2}{\eta_1}; \qquad \mu_2 = \frac{\eta_3}{\eta_1}; \qquad \mu_3 = \frac{\eta_4}{\eta_1}; \qquad \mu_4 = \frac{\eta_5}{\eta_1}; \qquad \mu_5 = \frac{\eta_6}{\eta_1} \tag{32}$$

with

$$\left.\begin{aligned}
\eta_1 &= sA_1 \\
\eta_2 &= b^2 A_2 + b^3 A_3 + 4b^2 sA_4 + b^2 fA_5 + b^2 gA_6 + 4b^2 A_7 + 2bA_8 + A_9 \\
\eta_3 &= 4b^2 sB_1 + 4b^3 tB_2 + b^2 fB_3 + 4aB_4 + 4b^2 B_5 + 4bcB_6 + 4beB_7 + 8bB_8 + 4cB_9 + C_1 \\
\eta_4 &= 4abC_2 + 4aC_3 + 4bcC_4 + C_5 + 4bC_6 + 4c^2 C_7 + 4cC_8 + 16eC_9 + D_1 \\
\eta_5 &= 4aD_2 + 4bD_3 + 4c^2 D_4 + 4cD_5 + D_6 \\
\eta_6 &= tD_7
\end{aligned}\right\} \tag{33}$$

where A_1–A_9, B_1–B_9 and C_1 –C_9 are defined in Appendix II.

The differential equation (31) is linear with constant coefficients so that the solution can be assumed in the form

$$X = X_0 e^{r\xi} \tag{34}$$

Substituting Eq. (34) into Eq. (31) gives the auxiliary equation as follow

$$\lambda^{10} + \mu_1 \lambda^8 + \mu_2 \lambda^6 + \mu_3 \lambda^4 + \mu_4 \lambda^2 + \mu_5 = 0 \tag{35}$$

The above equation is a quintic in $p = \lambda^2$, namely

$$p^5 + \mu_1 p^4 + \mu_2 p^3 + \mu_3 p^2 + \mu_4 p \;\; + \mu_5 = 0 \tag{36}$$

which can be solved in a routine way.

Some pair or pairs of complex roots may occur, but as U_1, U_3, Θ_1, Θ_3 and W are all real, the associated coefficients; say X_j in the solution for $X = \sum_{j=1}^{10} X_j e^{r_j \xi}$ will also be complex. As complex roots occur only in conjugate pairs, the associated X_j will also occur in conjugate pairs.

Thus, the solution for U_1, U_3, Θ_1, Θ_3 and W can be written as

$$U_1 = \sum_{j=1}^{10} P_j e^{r_j \xi} \; ; \; U_3 = \sum_{j=1}^{10} Q_j e^{r_j \xi} \; ; \; \Theta_1 = \sum_{j=1}^{10} R_j e^{r_j \xi} \; ; \; \Theta_3 = \sum_{j=1}^{10} S_j e^{r_j \xi} \; ; \; W = \sum_{j=1}^{10} T_j e^{r_j \xi} \tag{37}$$

where r_j (j = 1, 2…10) are the 10 roots of the auxiliary equation and P_j, Q_j, R_j, S_j and T_j, (j = 1,2…10) are five sets of ten, possibly complex, constants.

By substituting Eq. (37) into Eqs. (26)–(30) it can be shown that the constants P_j, Q_j, R_j and S_j are related to T_j as follows so that the responses U_1, U_3, Θ_1, Θ_3 and W are linear combination of T_j.

$$P_j = \alpha_j T_j ; \qquad Q_j = \beta_j T_j ; \qquad R_j = \gamma_j T_j ; \qquad S_j = \eta_j T_j \tag{38}$$

where $\alpha_j, \beta_j, \gamma_j$ and η_j can be expressed directly from the five differential equations (26)-(30) and by applying Cramer's rule to the following relationship for the determination of P_j, Q_j, R_j and S_j, see Appendix III.

$$\begin{bmatrix} \left(r_j^2 + a\right) & \left(br_j^2 + c\right) & h_1\left(br_j^2 + e\right) & -\frac{h_3}{2}\left(br_j^2 + c\right) \\ \left(br_j^2 + c\right) & \left(gr_j^2 + h\right) & \frac{h_1}{2}\left(br_j^2 + c\right) & -h_3\left(br_j^2 + e\right) \\ \left(br_j^2 + e\right) & \frac{1}{2}\left(br_j^2 + c\right) & h_1\left(zr_j^2 + m\right) & -\frac{h_3}{4}\left(br_j^2 + c\right) \\ -\frac{1}{2}\left(br_j^2 + c\right) & -\left(br_j^2 + e\right) & -\frac{h_1}{4}\left(br_j^2 + c\right) & h_3\left(pr_j^2 + q\right) \end{bmatrix} \times \begin{bmatrix} P_j \\ Q_j \\ R_j \\ S_j \end{bmatrix} = \begin{bmatrix} fr_j \\ -fr_j \\ -nr_j \\ rr_j \end{bmatrix} T_j \tag{39}$$

The expressions for the amplitudes of the axial forces in layer 1 and 3 (F_1 and F_3), the shear force across the cross-section (S) and the bending moments in layers 1 and 3 (M_1 and M_3) are given in Eqs. (20)–(24). With the help of Eqs. (37) and (38) it can be shown that the loads $F_1(\xi), F_3(\xi), M_1(\xi), M_3(\xi)$ and $S(\xi)$ are also linear combinations of T_j. Noting that these forces and moments vary harmonically during vibratory motion in the same way as the displacements and rotations, so that they are (as functions of the variable $\xi = x/L$) given by

$$\left.\begin{aligned} F_1(\xi) = \sum_{j=1}^{10} -\Bigg\{ & \frac{r_j\alpha_j}{L}\left(E_1A_1+\frac{1}{4}E_2A_2+\frac{1}{h_2^{\,2}}E_2I_2\right)+\frac{r_j\beta_j}{L}\left(\frac{1}{4}E_2A_2-\frac{1}{h_2^{\,2}}E_2I_2\right) \\ & +\frac{r_j\gamma_j}{L}\left(\frac{1}{8}h_1E_2A_2+\frac{h_1}{2h_2^{\,2}}E_2I_2\right)+\frac{r_j\eta_j}{L}\left(-\frac{1}{8}h_3E_2A_2+\frac{h_3}{2h_2^{\,2}}E_2I_2\right)\Bigg\} e^{r_j\xi}T_j \end{aligned}\right\} \quad (40)$$

$$\left.\begin{aligned} F_3(\xi) = \sum_{j=1}^{10} -\Bigg\{ & \frac{r_j\alpha_j}{L}\left(\frac{1}{4}E_2A_2-\frac{1}{h_2^{\,2}}E_2I_2\right)+\frac{r_j\beta_j}{L}\left(E_3A_3+\frac{1}{4}E_2A_2+\frac{1}{h_2^{\,2}}E_2I_2\right) \\ & +\frac{r_j\gamma_j}{L}\left(\frac{h_1}{8}E_2A_2-\frac{h_1}{2h_2^{\,2}}E_2I_2\right)+\frac{r_j\eta_j}{L}\left(-\frac{1}{8}h_3E_2A_2-\frac{h_3}{2h_2^{\,2}}E_2I_2\right)\Bigg\} e^{r_j\xi}T_j \end{aligned}\right\} \quad (41)$$

$$\left.\begin{aligned} M_1(\xi) = \sum_{j=1}^{10} -\Bigg\{ & \frac{r_j\alpha_j}{L}\left(\frac{h_1}{8}E_2A_2+\frac{h_1}{2h_2^{\,2}}E_2I_2\right)+\frac{r_j\beta_j}{L}\left(\frac{h_1}{8}E_2A_2-\frac{h_1}{2h_2^{\,2}}E_2I_2\right) \\ & +\frac{r_j\gamma_j}{L}\left(E_1I_1+\frac{h_1^{\,2}}{16}E_2A_2+\frac{h_1^{\,2}}{4h_2^{\,2}}E_2I_2\right)+\frac{r_j\eta_j}{L}\left(-\frac{h_1h_3}{16}E_2A_2+\frac{h_1h_3}{4h_2^{\,2}}E_2I_2\right)\Bigg\} e^{r_j\xi}T_j \end{aligned}\right\} \quad (42)$$

$$\left.\begin{aligned} M_3(\xi) = \sum_{j=1}^{10} -\Bigg\{ & \frac{r_j\alpha_j}{L}\left(-\frac{h_3}{8}E_2A_2+\frac{h_3}{2h_2^{\,2}}E_2I_2\right)+\frac{r_j\beta_j}{L}\left(-\frac{h_3}{8}E_2A_2-\frac{h_3}{2h_2^{\,2}}E_2I_2\right) \\ & +\frac{r_j\gamma_j}{L}\left(-\frac{h_1h_3}{16}E_2A_2+\frac{h_1h_3}{4h_2^{\,2}}E_2I_2\right)+\frac{r_j\eta_j}{L}\left(E_3I_3+\frac{h_3^{\,2}}{16}E_2A_2+\frac{h_3^{\,2}}{4h_2^{\,2}}E_2I_2\right)\Bigg\} e^{r_j\xi}T_j \end{aligned}\right\} \quad (43)$$

$$\left.\begin{aligned} S(\xi) = \sum_{j=1}^{10} -\Bigg\{ & \frac{r_j}{L}(k_1A_1G_1+k_2A_2G_2+k_3A_3G_3)+\alpha_j\left(\frac{k_2A_2G_2}{h_2}\right)-\beta_j\left(\frac{k_2A_2G_2}{h_2}\right) \\ & +\gamma_j\left(-k_1A_1G_1+\frac{h_1k_2A_2G_2}{2h_2}\right)+\eta_j\left(-k_3A_3G_3+\frac{h_3k_2A_2G_2}{2h_2}\right)\Bigg\} e^{r_j\xi}T_j \end{aligned}\right\} \quad (44)$$

2.2 Formulation of the dynamic stiffness matrix

The amplitudes of the responses and loads of the freely vibrating sandwich beam are given by Eqs. (37) and Eqs. (40)-(44), respectively which can now be related by the dynamic stiffness matrix on eliminating the arbitrary constants T_j (j = 1, 2, 3,….10). Referring to Fig. 2 the boundary conditions for responses and loads of the sandwich beam are as follows.

At the left hand end, $\xi = 0$ (x = 0), the responses are U_1 (0), U_3 (0), Θ_1 (0), Θ_3 (0) and W (0). The corresponding responses at the right hand end, $\xi = 1$ (x = L), are U_1 (1), U_3 (1), Θ_1 (1), Θ_3 (1) and W (1), see Fig. 2. By substituting $\xi = 0$ and $\xi = 1$ in Eq (37), these boundary conditions give

$$U_1(0) = \sum_{j=1}^{10} P_j \; ; \; U_3(0) = \sum_{j=1}^{10} Q_j \; ; \; \Theta_1(0) = \frac{1}{L}\sum_{j=1}^{10} R_j \; ; \; \Theta_3(0) = \frac{1}{L}\sum_{j=1}^{10} S_j \; ; \; W(0) = \sum_{j=1}^{10} T_j \tag{45}$$

$$U_1(1) = \sum_{j=1}^{10} P_j e^{r_j} \; ; U_3(1) = \sum_{j=1}^{10} Q_j e^{r_j} \; ; \quad \Theta_1(1) = \frac{1}{L}\sum_{j=1}^{10} R_j e^{r_j} \; ; \Theta_3(1) = \frac{1}{L}\sum_{j=1}^{10} S_j e^{r_j} \; ; \; W(1) = \sum_{j=1}^{10} T_j e^{r_j} \tag{46}$$

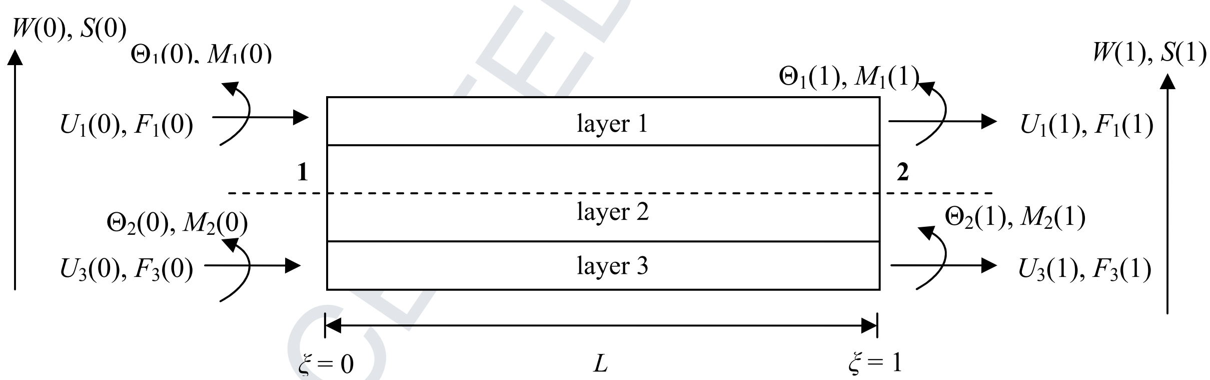

Fig. 2. End conditions for responses and loads for the three-layered sandwich beam

Equations (45) and (46) can be written in the following matrix form and by using Eq. (38) and simply referring the state vector of response $U_1(0)$, U_3 (0), Θ_1 (0), Θ_3 (0), W (0), U_1 (1), U_3 (1), Θ_1 (1), Θ_3 (1) and W (1), to only one set of arbitrary constants T_j as follows.

$$\begin{bmatrix} U_1(0) \\ U_3(0) \\ \Theta_1(0) \\ \Theta_3(0) \\ W(0) \\ U_1(1) \\ U_3(1) \\ \Theta_1(1) \\ \Theta_3(1) \\ W(1) \end{bmatrix} = \begin{bmatrix} \alpha_1 & \alpha_2 & \alpha_3 & \alpha_4 & \alpha_5 & \alpha_6 & \alpha_7 & \alpha_8 & \alpha_9 & \alpha_{10} \\ \beta_1 & \beta_2 & \beta_3 & \beta_4 & \beta_5 & \beta_6 & \beta_7 & \beta_8 & \beta_9 & \beta_{10} \\ \gamma_1 & \gamma_2 & \gamma_3 & \gamma_4 & \gamma_5 & \gamma_6 & \gamma_7 & \gamma_8 & \gamma_9 & \gamma_{10} \\ \eta_1 & \eta_2 & \eta_3 & \eta_4 & \eta_5 & \eta_6 & \eta_7 & \eta_8 & \eta_9 & \eta_{10} \\ 1 & 1 & 1 & 1 & 1 & 1 & 1 & 1 & 1 & 1 \\ \alpha_1 e^{r1} & \alpha_2 e^{r2} & \alpha_3 e^{r3} & \alpha_4 e^{r4} & \alpha_5 e^{r5} & \alpha_6 e^{r6} & \alpha_7 e^{r7} & \alpha_8 e^{r8} & \alpha_9 e^{r9} & \alpha_{10} e^{r10} \\ \beta_1 e^{r1} & \beta_2 e^{r2} & \beta_3 e^{r3} & \beta_4 e^{r4} & \beta_5 e^{r5} & \beta_6 e^{r6} & \beta_7 e^{r7} & \beta_8 e^{r8} & \beta_9 e^{r9} & \beta_{10} e^{r10} \\ \gamma_1 e^{r1} & \gamma_2 e^{r2} & \gamma_3 e^{r3} & \gamma_4 e^{r4} & \gamma_5 e^{r5} & \gamma_6 e^{r6} & \gamma_7 e^{r7} & \gamma_8 e^{r8} & \gamma_9 e^{r9} & \gamma_{10} e^{r10} \\ \eta_1 e^{r1} & \eta_2 e^{r2} & \eta_3 e^{r3} & \eta_4 e^{r4} & \eta_5 e^{r5} & \eta_6 e^{r6} & \eta_7 e^{r7} & \eta_8 e^{r8} & \eta_9 e^{r9} & \eta_{10} e^{r10} \\ e^{r1} & e^{r2} & e^{r3} & e^{r4} & e^{r5} & e^{r6} & e^{r7} & e^{r8} & e^{r9} & e^{r10} \end{bmatrix} \times \begin{bmatrix} T_1 \\ T_2 \\ T_3 \\ T_4 \\ T_5 \\ T_6 \\ T_7 \\ T_8 \\ T_9 \\ T_{10} \end{bmatrix} \quad (47)$$

or

$$\boldsymbol{\delta} = \mathbf{Q}\,\mathbf{T} \quad (48)$$

where δ and **T** are displacement and constant vectors respectively and **Q** is the 10×10 square matrix given above.

Similarly at the left hand end, $\xi = 0\,(x = 0)$, the loads are F_1 (0), F_3 (0), M_1 (0), M_3 (0) and S (0), and the corresponding loads at the right hand end at $\xi = 1\,(x = L)$, are F_1 (1), F_3 (1), M_1 (1), M_3 (1) and S (1), see Fig. 2. By substituting $\xi = 0$ and 1 in Eqs. (40)-(44), and noting that the signs for the forces must be reversed at the right hand end and as a consequence of the convention, these boundary conditions give the following matrix relationship.

$$\begin{bmatrix} F_{11} \\ F_{31} \\ M_{11} \\ M_{31} \\ S_1 \\ F_{12} \\ F_{32} \\ M_{12} \\ M_{32} \\ S_2 \end{bmatrix} = \begin{bmatrix} a_{11} & a_{12} & a_{13} & a_{14} & a_{15} & a_{16} & a_{17} & a_{18} & a_{19} & a_{110} \\ a_{21} & a_{22} & a_{23} & a_{24} & a_{25} & a_{26} & a_{27} & a_{28} & a_{29} & a_{210} \\ a_{31} & a_{32} & a_{33} & a_{34} & a_{35} & a_{36} & a_{37} & a_{38} & a_{39} & a_{310} \\ a_{41} & a_{42} & a_{43} & a_{44} & a_{45} & a_{46} & a_{47} & a_{48} & a_{49} & a_{410} \\ a_{51} & a_{52} & a_{53} & a_{54} & a_{55} & a_{56} & a_{57} & a_{58} & a_{59} & a_{510} \\ a_{61} & a_{62} & a_{63} & a_{64} & a_{65} & a_{66} & a_{67} & a_{68} & a_{69} & a_{610} \\ a_{71} & a_{72} & a_{73} & a_{74} & a_{75} & a_{76} & a_{77} & a_{78} & a_{79} & a_{710} \\ a_{81} & a_{82} & a_{83} & a_{84} & a_{85} & a_{86} & a_{87} & a_{88} & a_{89} & a_{810} \\ a_{91} & a_{92} & a_{93} & a_{94} & a_{95} & a_{96} & a_{97} & a_{98} & a_{99} & a_{910} \\ a_{101} & a_{102} & a_{103} & a_{104} & a_{105} & a_{106} & a_{107} & a_{108} & a_{109} & a_{1010} \end{bmatrix} \times \begin{bmatrix} T_1 \\ T_2 \\ T_3 \\ T_4 \\ T_5 \\ T_6 \\ T_7 \\ T_8 \\ T_9 \\ T_{10} \end{bmatrix} \tag{49}$$

or

$$\mathbf{F} = \mathbf{RT} \tag{50}$$

where **F** is the state vector of loads, **T** is the vector of constants and the elements of the 10×10 square matrix **R** are as follows.

$$\left.\begin{aligned} a_{1j} = &-\frac{r_j\alpha_j}{L}\left(E_1A_1 + \frac{1}{4}E_2A_2 + \frac{1}{h_2{}^2}E_2I_2\right) - \frac{r_j\beta_j}{L}\left(\frac{1}{4}E_2A_2 - \frac{1}{h_2{}^2}E_2I_2\right) \\ &-\frac{r_j\gamma_j}{L}\left(\frac{1}{8}h_1E_2A_2 + \frac{h_1}{2h_2{}^2}E_2I_2\right) - \frac{r_j\eta_j}{L}\left(-\frac{1}{8}h_3E_2A_2 + \frac{h_3}{2h_2{}^2}E_2I_2\right) \end{aligned}\right\} \tag{51}$$

$$\left.\begin{aligned} a_{2j} = &-\frac{r_j\alpha_j}{L}\left(\frac{1}{4}E_2A_2 - \frac{1}{h_2{}^2}E_2I_2\right) - \frac{r_j\beta_j}{L}\left(E_3A_3 + \frac{1}{4}E_2A_2 + \frac{1}{h_2{}^2}E_2I_2\right) \\ &-\frac{r_j\gamma_j}{L}\left(\frac{h_1}{8}E_2A_2 - \frac{h_1}{2h_2{}^2}E_2I_2\right) - \frac{r_j\eta_j}{L}\left(-\frac{1}{8}h_3E_2A_2 - \frac{h_3}{2h_2{}^2}E_2I_2\right) \end{aligned}\right\} \tag{52}$$

$$\left.\begin{aligned} a_{3j} = &-\frac{r_j\alpha_j}{L}\left(\frac{h_1}{8}E_2A_2 + \frac{h_1}{2h_2{}^2}E_2I_2\right) - \frac{r_j\beta_j}{L}\left(\frac{h_1}{8}E_2A_2 - \frac{h_1}{2h_2{}^2}E_2I_2\right) \\ &-\frac{r_j\gamma_j}{L}\left(E_1I_1 + \frac{h_1{}^2}{16}E_2A_2 + \frac{h_1{}^2}{4h_2{}^2}E_2I_2\right) - \frac{r_j\eta_j}{L}\left(-\frac{h_1h_3}{16}E_2A_2 + \frac{h_1h_3}{4h_2{}^2}E_2I_2\right) \end{aligned}\right\} \tag{53}$$

$$\left.\begin{aligned} a_{4j} = &-\frac{r_j\alpha_j}{L}\left(-\frac{h_3}{8}E_2A_2 + \frac{h_3}{2h_2{}^2}E_2I_2\right) - \frac{r_j\beta_j}{L}\left(-\frac{h_3}{8}E_2A_2 - \frac{h_3}{2h_2{}^2}E_2I_2\right) \\ &-\frac{r_j\gamma_j}{L}\left(-\frac{h_1h_3}{16}E_2A_2 + \frac{h_1h_3}{4h_2{}^2}E_2I_2\right) - \frac{r_j\eta_j}{L}\left(E_3I_3 + \frac{h_3{}^2}{16}E_2A_2 + \frac{h_3{}^2}{4h_2{}^2}E_2I_2\right) \end{aligned}\right\} \tag{54}$$

$$\left.\begin{aligned} a_{5j} &= -\frac{r_j}{L}\left(k_1A_1G_1 + k_2A_2G_2 + k_3A_3G_3\right) - \alpha_j\left(\frac{k_2A_2G_2}{h_2}\right) + \beta_j\left(\frac{k_2A_2G_2}{h_2}\right) \\ &\quad - \gamma_j\left(-k_1A_1G_1 + \frac{h_1k_2A_2G_2}{2h_2}\right) - \eta_j\left(-k_3A_3G_3 + \frac{h_3k_2A_2G_2}{2h_2}\right) \end{aligned}\right\} \quad (55)$$

$$a_{6j} = -a_{1j}e^{r_j}\,; \quad a_{7j} = -a_{2j}e^{r_j}\,; \quad a_{8j} = -a_{3j}e^{r_j}\,; \quad a_{9j} = -a_{4j}e^{r_j}\,; \quad a_{10j} = -a_{5j}e^{r_j} \quad (56)\text{-}(60)$$

where $j = 1, 2, 3, \ldots\ldots\ldots.10$.

The dynamic stiffness matrix can now be formulated by eliminating **T** from the Eqs. (48) and (50) to give

$$\mathbf{F} = \mathbf{R}\,\mathbf{Q}^{-1}\boldsymbol{\delta} = \mathbf{K}\,\boldsymbol{\delta} \quad (61)$$

where

$$\mathbf{K} = \mathbf{R}\,\mathbf{Q}^{-1} \quad (62)$$

is the require dynamic stiffness matrix.

3. Application of the Dynamic Stiffness Matrix and Numerical Results

The above dynamic stiffness matrix can now be used to compute the natural frequencies and mode shapes of either a single three-layered sandwich beam or an assembly of such beams, for example a continuous sandwich beam on multiple supports. An accurate and reliable method of calculating the natural frequencies and mode shapes is to apply the algorithm of Wittrick and Williams (Banerjee, 2003; Banerjee and Sobey, 2005; Wittrick and Williams, 1971) to the dynamic stiffness matrix. The algorithm, unlike its proof, is simple to use and relies principally on the Sturm sequence property of the dynamic stiffness to converge on any natural frequency with certainty. It has featured in literally hundreds of papers the details of which are not repeated here, but for further insight interested readers are referred to the original work of Wittrick and Williams (1971).

First of all, for illustrative purposes two examples of a three-layered sandwich beam are provided to compare results obtained from the present theory to the ones computed using earlier (and simpler) theories. The first example is a three-layered sandwich beam of length 0.5m with rectangular cross-section. The top and bottom layers are made of steel with thicknesses 15 mm and 10mm respectively, whereas the middle layer is of rubber material with thickness 20 mm. The width is 40 mm for all layers. The properties used for steel and rubber are as follows with the suffix *s* denoting the properties for steel and the suffix *r* denoting the properties for rubber: $E_s = 210GPa$, $G_s = 80GPa$, $\rho_s = 7850kg/m^3$, $E_r = 1.5MPa$, $G_r = 0.5MPa$ and $\rho_r = 950kg/m^3$. The shear correction or shape factor used in the analysis for each layer is set to 2/3 which is generally used for a rectangular cross-section. The second example is similar to the first one except that only the central layer (i.e. the core) which was rubber in the first example, is now replaced by lead with material properties (using suffix *l*): $E_l = 16GPa$, $G_l = 5.5GPa$ and $\rho_l = 11100kg/m^3$.

The complete set of data used in the analysis for the two illustrative examples is shown in Table 1 for interested readers who wish to develop the present theory further or wish to check their own theories. The first four natural frequencies of the two examples, with cantilever end conditions, are shown in Table 2 together with the results obtained by using the earlier theory of Banerjee and Sobey (2005). The differences in the natural frequencies are quite small. This is to be expected because of the relatively important role played by the core, which is modelled as a Timoshenko beam both in the present theory as well as in the earlier theory of Banerjee and Sobey (2005). The main difference between the present theory and the earlier theory is essentially in the modelling of the top and bottom layers for which the effects of both shear deformation and rotatory inertia are included in the present theory, whereas only the effects of rotatory inertia are included in the earlier theory. For the results of the two examples shown in Table 2, shear deformation of the face layers is not expected to have any major effect.

Figures 3 and 4 illustrate the first four natural frequencies and mode shapes of the two cantilever sandwich beams. The results reveal some interesting features. For the first example the modes are all dominated by flexure (W displacement). This occurs because of the soft core and strong face materials. The fundamental mode exhibits flexural displacement associated with small axial displacements (U_1 and U_3) of the face layers that are moving in opposite directions. The second and third modes have similar trends, but the fourth mode is a pure flexural one. In the second example, where the central core is replaced by lead, the first three modes are similar to the ones shown for the first example so that the free vibratory motion is predominantly flexural. However, the fourth mode is purely axial with U_1 and U_3 displacements in the same direction, but no flexural motion. (Note that the two graphs shown in Fig. 4 for U_1 and U_3 in the fourth mode are coincident.) This is in sharp contrast to the fourth mode of the first example. The high density and low Young's modulus of lead used for the core in the second example is the main reason for this type of mode. This is in accord with the earlier investigation carried out by Banerjee and Sobey (2005).

The next set of results was obtained to illustrate the effects of shear deformation and rotary inertia on the natural frequencies of the sandwich beams. To demonstrate these effects, the length of the beam was varied and the natural frequencies of the two examples were computed and plotted against of h/L, where $h = h_1 + h_2 + h_3$ is the total thickness of the sandwich beam. For the above two examples, Figures 5(a) and 5(b) show results obtained for the first two natural frequencies. The percentage error shown is calculated relative to the case when the effects of shear deformation and rotary inertia of the top and bottom layers are both neglected. The natural frequencies denoted by ω_i (i = 1 and 2) correspond to the cases when the effects are ignored whereas the ones denoted by ω_i^* include the effects. When h/L increases the error also increases, as expected. The magnitudes of the error for the two examples are different for the first natural frequency, but similar for the second one. The maximum error is around 9 % in the second natural frequency for both cases when the thickness to length ratio is around 0.5.

Table 1

Data used for computation of natural frequencies and mode shapes of examples 1 and 2

Properties	Layer 1 (Steel)	Layer 2 (Rubber) Example 1	Layer 2 (Lead) Example 2	Layer 3 (Steel)
b (m)	0.04	0.04	0.04	0.04
h (m)	0.015	0.02	0.02	0.01
A (m^2)	0.0006	0.0008	0.0008	0.0004
I (m^4)	1.125×10^{-08}	2.67×10^{-08}	2.67×10^{-08}	3.33×10^{-09}
G (GPa)	80	0.0005	5.5	80
E (GPa)	210	0.0015	16	210
ρ (kg/m^3)	7850	950	11100	7850
k	2/3	2/3	2/3	2/3
EA (N)	1.26×10^{8}	1.20×10^{3}	1.28×10^{7}	8.40×10^{7}
EI (Nm^2)	2.36×10^{3}	4.00×10^{-2}	4.27×10^{2}	7.00×10^{2}
kAG (N)	3.20×10^{7}	2.67×10^{3}	2.93×10^{6}	2.13×10^{7}
ρA (kg/m)	4.71	0.76	8.88	3.14
ρI (kgm)	8.83125×10^{-5}	2.53×10^{-5}	0.000296	2.62×10^{-5}
L (m)	0.5	0.5	0.5	0.5

Table 2

Natural frequencies of a three-layered sandwich beam with cantilever end conditions

Frequency No.	Natural frequencies (rad/s)			
	Example 1		Example 2	
	Using Banerjee and Sobey (2005)	Present Theory	Using Banerjee and Sobey (2005)	Present Theory
1	291.687	291.50	776.09	776.4
2	1691.39	1684.48	3880.57	3841.1
3	4669.07	4623.98	8899.37	8753.1
4	9104.77	8945.18	11461.7	11459.2

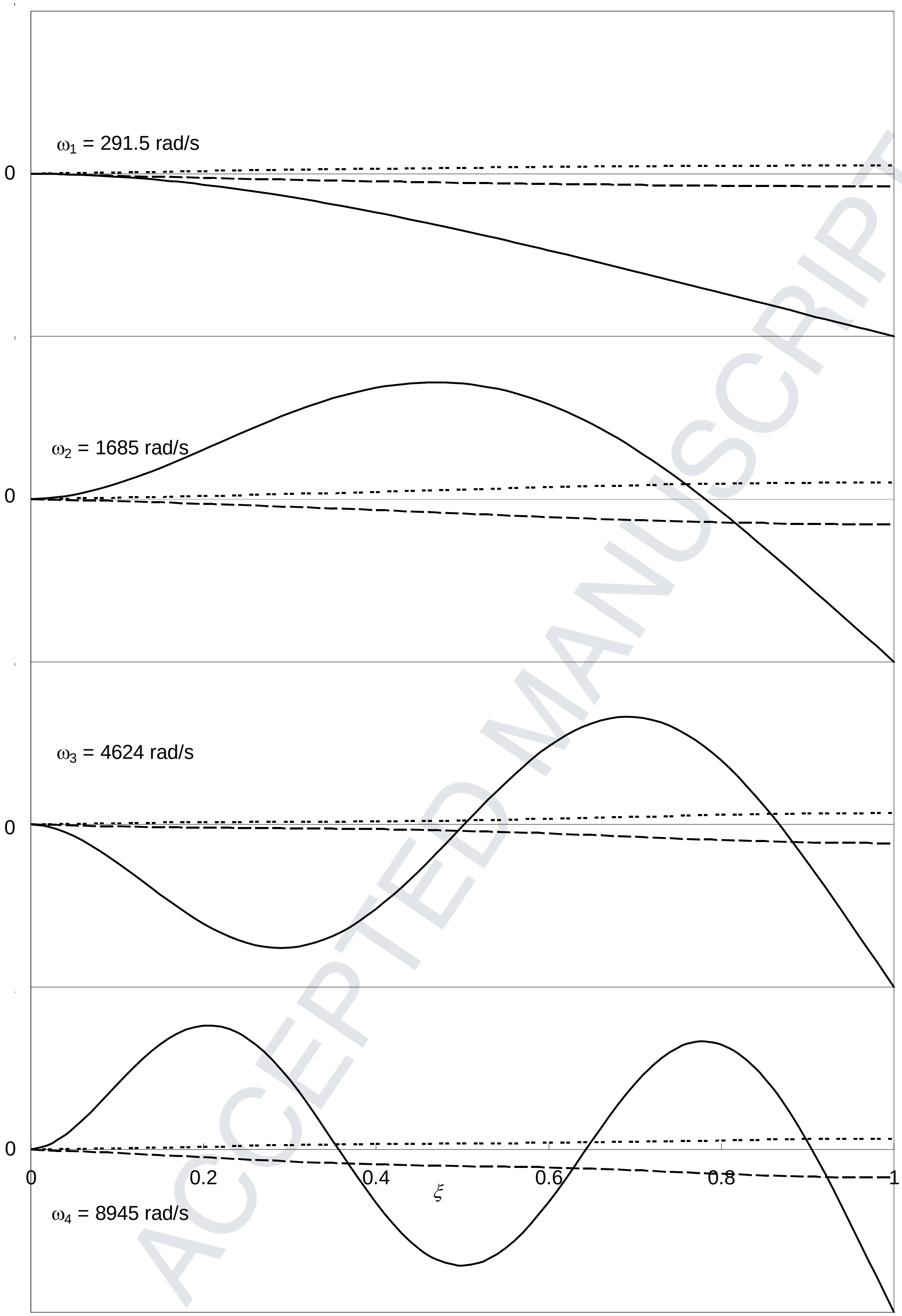

Fig.3. Natural frequencies and mode shapes of the three-layered sandwich beam of example 1. ———— W; - - - - - - - - - - U_1; -·-·-·-·-·- U_3

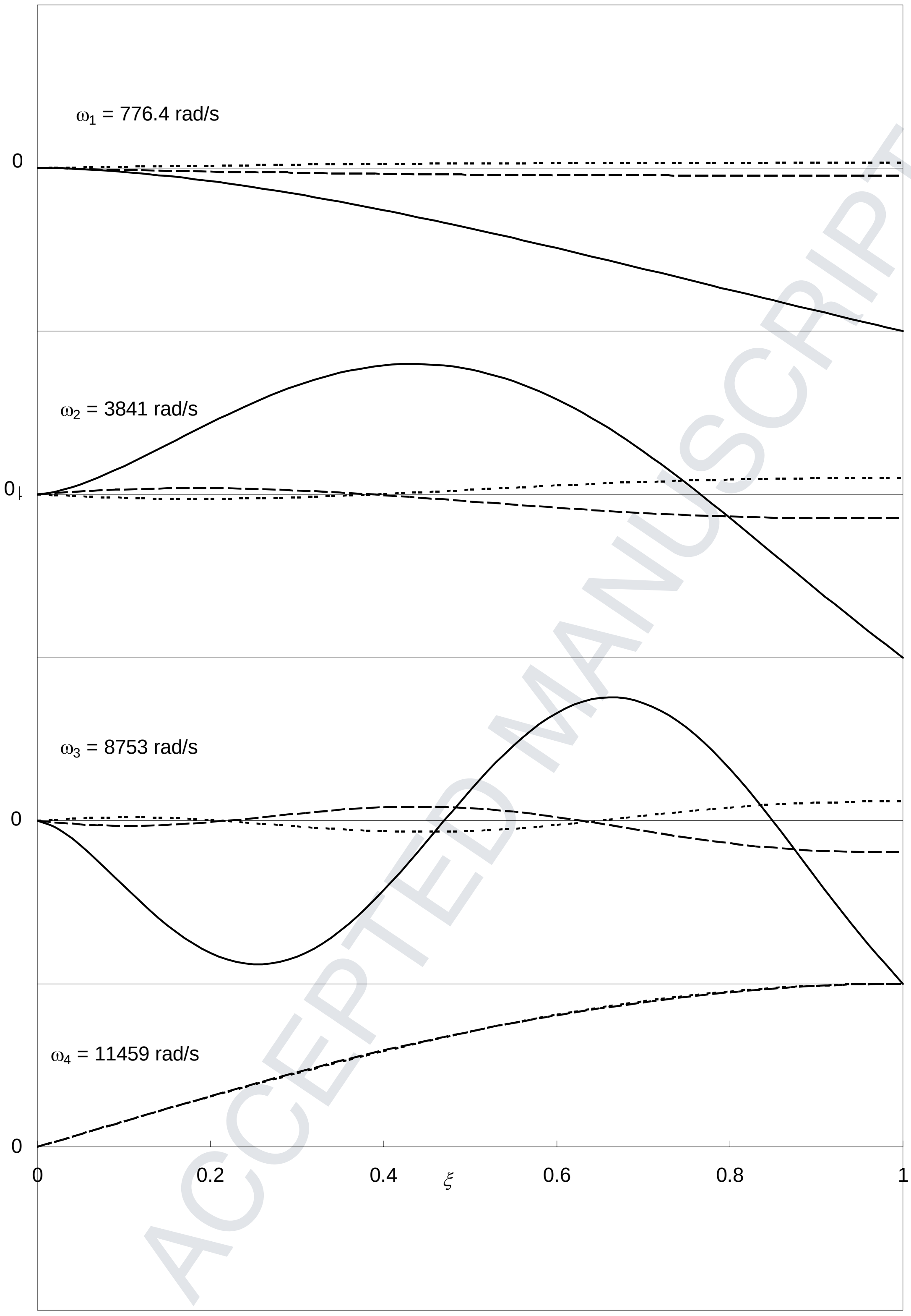

Fig. 4. Natural frequencies and mode shapes of the three-layered sandwich beam of example 2. ———— W; - - - - - - U_1; -·-·-·-·- U_3

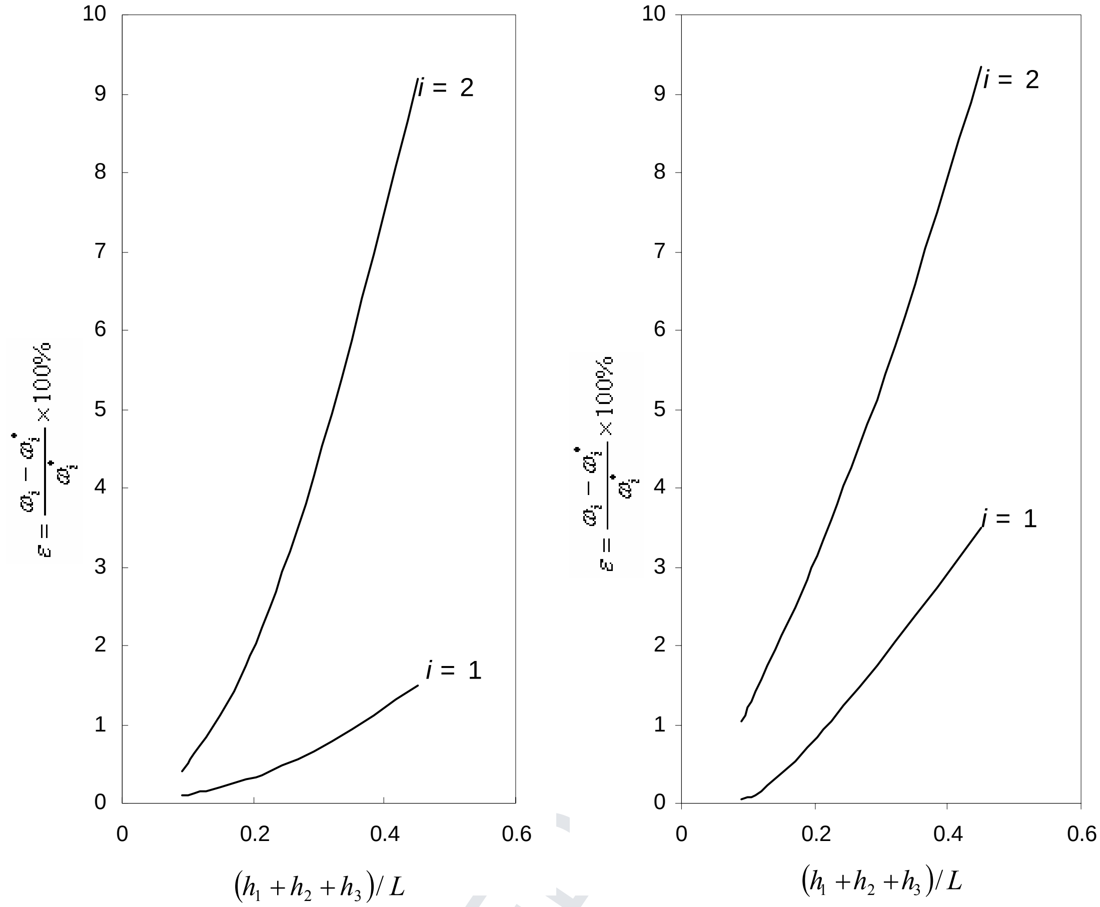

(a) Example 1

(b) Example 2

Fig.5. Effect of thickness to length ratio on the natural frequencies of examples 1and 2.

4. Modal Testing and Further Validation of the Theory

Experimental measurements of natural frequencies of three sandwich beam samples have been carried out using an impulse hammer kit with its associated software for data capturing and analysis. The beam samples are fabricated from aluminium, steel and rubber sheets that are pre-treated and polished first. Later they are degreased using acetone for 2 minutes before applying the adhesive (Araldite 2011). The surfaces are then dried and the adhesive applied evenly using a glue gun on the rubber surface, and the metal skin is laid on top for each side at a time. This is repeated for the other side of the rubber after allowing for 24 hours of curing time. Once the adhesive is applied the sandwich samples are cured for a further period of 24 hours in a press. Basically, the samples are laid on the base of the press between two thick metal plates to ensure pressure is distributed evenly all through the structure. The finished products are (with thicknesses shown in parentheses): (i) aluminium (2 mm)–rubber (18 mm)–aluminium (2 mm), (ii) steel (1.5 mm)–rubber (18 mm)–steel (2.4 mm), and (iii) steel (1.5 mm)–rubber (18 mm)–aluminium (2 mm), sandwich beams of length 500 mm and width 50 mm for each.

The experimental modal testing set up using the impact hammer kit consisting of a PC driven ACE dynamic signal analyser and an accelerometer is shown in Fig. 6. All test specimens were cantilevered with one end fully built-in in order to prevent all displacements. The accelerometer is set at a fixed position on the test specimen, which is considered to be the reference point while the impact hammer is used at a number of points to generate the excitation forces on the test specimen, corresponding to the degrees of freedom allowed in the model. The location of the driving and measurement points is carefully chosen to identify all important modes of vibration of the structure within the desired frequency range. The transfer function between the driving force and the resulting response is computed using the data obtained during the measurement. Sandwich test specimens are excited at specified grid points that define the number of degrees of freedom of the structure. The Dynamic Signal Analyser system is used to extract force and signal response from the structure under test. The response signals recorded by the accelerometer attached to the test specimen and the force signals recorded by the force transducer fitted inside the hammerhead are averaged from three repeated excitations and measurements at each location. The signal analyser further processes these signals and the frequency response functions (FRFs) are plotted against frequency from which the natural frequencies are identified. The first three measured natural frequencies of the above three specimens (except for the third natural frequency of sample 3 which apparently did not show any peak) are shown in Table 3 alongside those calculated using the present theory. The variation of results between the theory and experiment is noticeable. The maximum difference is as much as 19%. The discrepancy is rather large and in part, can be attributed to the fact that the properties of rubber used in the theoretical analysis were not sufficiently accurate to match the ones used in the experiments. It is well known that the properties of rubber can vary markedly, but unfortunately the authors were unable to pinpoint the properties used in the experimental samples, accurately. Furthermore, a few difficulties were also encountered when carrying out the experiment, particularly when applying the built-in boundary condition at one end of the sandwich beam.

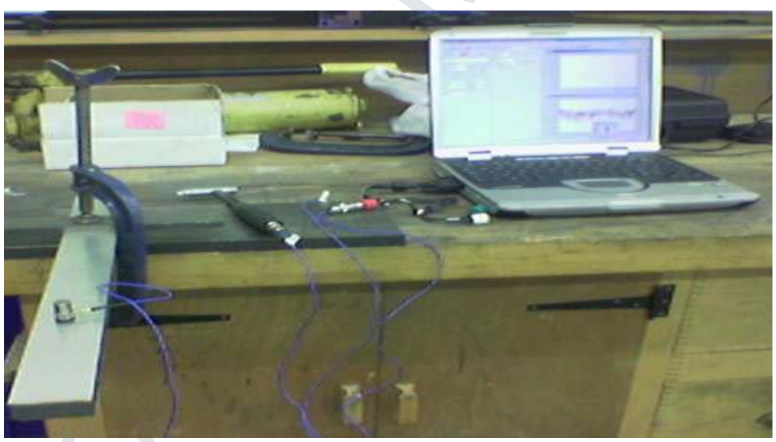

Fig. 6 Experimental set up for modal testing of a cantilever sandwich beam.

As an acceptable alternative, the authors carried out further investigations on fixed-fixed sandwich beams for which some experimental results reported in the literature came to their notice, see Raville et al (1961). This enabled further comparison of results to be possible. The results from the present theory and the experimental results of Raville et al (1961) are shown in Table 4 together with the theoretical results recently published by Howson and Zare (2005). Note that Howson and Zare (2005) also reported the experimental results of Raville et al (1961) alongside their own theoretical results, but the volume number they quoted for this reference is in error (it should be 28 instead of 83). The data used for this sandwich beam with length L = 1.2187 m are (see Howson and Zare (2005))

$E_1 = E_3$ = 68.9 GPa, E_2 = 179.14 MPa, $G_1 = G_3$ = 26.5 GPa, G_2 = 68.9 MPa, $\rho_1 = \rho_3$ = 2687.3 kg/m^3, ρ_2 = 119.69 kg/m^3, $h_1 = h_3$ = 0.40624 mm, h_2 = 6.3475 mm, $b_1 = b_2 = b_3$ = 25.4 mm, $k_1 = k_2 = k_3$ = 2/3.

It should be noted that Raville et al (1961) in their experimental work, were able to measure only those natural frequencies of the sandwich beam that were above 100 Hz. This limitation was due to the equipment that was available to them at the time. As a consequence, they were unable to determine the first two natural frequencies of the sandwich beam. (The vibration exciter they used was not capable of generating a forcing function of the proper magnitude and frequency to capture the first two natural frequencies.) As shown in Table 4, the agreement between the set of results using the present theory, the experimental results of Raville et al (1961) and the theoretical results of Howson and Zare (2005) is generally very good. The maximum discrepancy is around 8%. Given the complexity of the problem and difficulties in the experimentation, this discrepancy is judged to be acceptable and within engineering accuracy.

Table 3

Experimental and theoretical natural frequencies of a three-layered sandwich beam

Sandwich beam specimens	Frequency no (i)	Natural frequencies (Hz)		% difference with experiment
		Experiment	Present theory	
(i) Aluminium-Rubber-Aluminium	1	11.25	10.46	7.02
	2	33.75	36.31	7.59
	3	93.75	75.94	19.0
(ii) Steel-Rubber-Steel	1	10.62	9.04	14.9
	2	29.38	33.88	15.3
	3	53.75	63.73	18.6
(iii) Steel-Rubber-Aluminium	1	10.63	9.45	11.1
	2	29.38	33.30	13.3
	3	-	70.74	-

Table 4

Comparative results for the first seven natural frequencies of a fixed-fixed sandwich beam

Frequency no	Natural frequency (Hz)		
	Present theory	Experimental results Raville et al (1961)	Howson and Zare (2005)
1	34.342	–	34.597
2	91.385	–	93.100
3	171.69	185.5	177.16
4	270.36	280.3	282.78
5	383.27	399.4	406.33
6	506.88	535.2	544.33
7	638.39	680.7	693.79

5. Limitations of the Theory and Scope for Further Research

The type of sandwich beam considered in this paper consists of structural face sheets rigidly bonded to a stabilizing core, which can have markedly different properties. Only the transverse vibration coupled with longitudinal deformation is considered and no allowances are made for lateral and/or torsional displacements. Clearly, the displacement field within the sandwich beam, particularly in the vicinity of the interface (junction), will be quite complex. The formulation presented here does not account for the higher order effects caused by the nonlinearity of the longitudinal and transverse deformations of the face layers and core through their thicknesses. Also the theory is compromised by ignoring the effect of warping of the cross-section caused by shear stresses. It has been assumed that the whole cross-section of the sandwich beam remains plane during flexure so that the displacements vary linearly through the thicknesses, which is, no-doubt a serious restriction. Although the dynamic stiffness theory presented here provides some practical advantages, a more detailed analytical approach based on rigorous three-dimensional mathematical theory of elasticity might be useful particularly when the material properties change abruptly and the thicknesses of the face layers and core are relatively large. In this respect papers on the applications of zig-zag theories published by Icardi (2001, 2003) are worthy of careful study. In future research the face layers may be replaced by laminated composites.

6. Conclusions

An accurate dynamic stiffness matrix for a three-layered sandwich beam of asymmetric cross-section has been developed using Timoshenko beam theory, Hamiltonian mechanics and symbolic computation. The resulting dynamic stiffness matrix is applied using Wittrick-Williams algorithm to compute the natural frequencies and mode shapes of some illustrative examples. The results agree very well with those obtained using the earlier theories. An impulse hammer test has been carried out on three different sandwich beam samples and the experimental results match reasonably well with theoretical predictions using the dynamic stiffness theory. The investigation provides optimism for future studies on the dynamic analysis of complex sandwich structural systems.

Appendix I : Non-dimensional sandwich beam parameters used in Eqs. (26)-(30)

$$a=-\frac{K_2A_2G_2L^2}{h_2{}^2\left(E_1A_1+\frac{E_2A_2}{3}\right)}+\frac{\left(\rho_1A_1+\frac{\rho_2A_2}{3}\right)}{\left(E_1A_1+\frac{E_2A_2}{3}\right)}L^2\omega^2,$$

$$b=\frac{\frac{E_2A_2}{6}}{\left(E_1A_1+\frac{E_2A_2}{3}\right)},$$

$$c=\frac{k_2A_2G_2L^2}{h_2{}^2\left(E_1A_1+\frac{E_2A_2}{3}\right)}+\frac{\left(\frac{\rho_2A_2}{6}\right)}{\left(E_1A_1+\frac{E_2A_2}{3}\right)}L^2\omega^2,$$

$$e=-\frac{\frac{k_2A_2G_2}{2h_2{}^2}L^2}{\left(E_1A_1+\frac{E_2A_2}{3}\right)}+\frac{\left(\frac{\rho_2A_2}{6}\right)}{\left(E_1A_1+\frac{E_2A_2}{3}\right)}L^2\omega^2,$$

$$f=\frac{k_2A_2G_2L}{h_2\left(E_1A_1+\frac{E_2A_2}{3}\right)},$$

$$g=\frac{E_3A_3+\frac{E_2A_2}{3}}{\left(E_1A_1+\frac{E_2A_2}{3}\right)},$$

$$h=-\frac{k_2A_2G_2L^2}{h_2{}^2\left(E_1A_1+\frac{E_2A_2}{3}\right)}+\frac{\left(\rho_3A_3+\frac{\rho_2A_2}{3}\right)}{\left(E_1A_1+\frac{E_2A_2}{3}\right)}L^2\omega^2,$$

$$m=-\frac{\left(k_1A_1G_1+\frac{h_1{}^2K_2A_2G_2}{4h_2{}^2}\right)L^2}{\left(E_1A_1+\frac{E_2A_2}{3}\right)h_1{}^2}+\frac{\left(\rho_1I_1+\frac{\rho_2A_2h_1{}^2}{12}\right)}{\left(E_1A_1+\frac{E_2A_2}{3}\right)h_1{}^2}L^2\omega^2,$$

$$n=\frac{\left\{k_1A_1G_1-\left(\frac{k_2A_2G_2h_1}{2h_2}\right)\right\}L}{\left(E_1A_1+\frac{E_2A_2}{3}\right)h_1},$$

$$p=\frac{E_3I_3+\left(\frac{E_2A_2h_3{}^2}{12}\right)}{\left(E_1A_1+\frac{E_2A_2}{3}\right)h_3{}^2},$$

$$q=-\frac{\left\{\left(\frac{k_2A_2G_2h_3{}^2}{4h_2{}^2}\right)+k_3A_3G_3\right\}L^2}{\left(E_1A_1+\frac{E_2A_2}{3}\right)h_3{}^2}+\frac{\left\{\left(\frac{\rho_2A_2h_3{}^2}{12}\right)+\rho_3I_3\right\}}{\left(E_1A_1+\frac{E_2A_2}{3}\right)h_3{}^2}L^2\omega^2,$$

$$r=\frac{\left\{\left(\frac{k_2A_2G_2h_3}{2h_2}\right)-k_3A_3G_3\right\}L}{\left(E_1A_1+\frac{E_2A_2}{3}\right)h_3},$$

$$s=\frac{k_1A_1G_1+k_2A_2G_2+k_3A_3G_3}{\left(E_1A_1+\frac{E_2A_2}{3}\right)},$$

$$t=\frac{(\rho_1A_1+\rho_2A_2+\rho_3A_3)L^2\omega^2}{\left(E_1A_1+\frac{E_2A_2}{3}\right)},$$

$$z=\frac{E_1I_1+\left(\frac{E_2A_2h_1{}^2}{12}\right)}{\left(E_1A_1+\frac{E_2A_2}{3}\right)h_1{}^2}.$$

Appendix II : Non-dimensional sandwich beam parameters used in Eqs. (33)

$$A_1 = (-4b^3g-16b^3p-16b^3z-4b^3+16b^2gp+4b^2gz+b^2g+16b^2pz+4b^2p+16b^2z-16gpz)$$

$$A_2 = ags + 4aps + 16asz$$

$$A_3 = -4as + 32cs - 32es - 16f^2 + 32fn - 32fr - 4gt - 4hs - 16ms - 16n^2 + 32nr - 16pt - 16qs - 16r^2 - 16tz - 4t$$

$$A_4 = -2cg - 8cp - 8cz - 2c - eg - 4ep - 4ez - e + 4hp + hz + 0.25h + 4mp + 4m + 4qz + q$$

$$A_5 = fg + 36fp + 36fz + f + 4gn + 8gr - 16np - 8n + 16rz - 4r$$

$$A_6 = 4ms + 4n^2 - 16nr + 16pt + 16qs + 16r^2 + 4tz + t$$

$$A_7 = 4n^2p + 4n^2 - 4nr + 4ptz + pt + 4r^2z + r^2 + 4tz$$

$$A_8 = 4cgsz + cgs + 16cpsz + 4cps + 16egps + 16esz - 16f^2pz - 16fgnp - 8fgrz + 8fnp + 16frz + 4gnr$$

$$A_9 = -16agpsz - 16f^2gpz - 16f^2pz - 16gmps - 16gn^2p - 16gptz - 16gqsz - 16gr^2z - 16hpsz$$

$$B_1 = -2ac - ae + 0.25ah + 4am + aq + 4c^2 + 16ce - 2ch - 8cm - 8cq - 20e^2 - eh - 4em - 4eq + hm + 4hq + 4mq$$

$$B_2 = -a + 8c - 8e - h - 4m - 4q$$

$$B_3 = af - 8an - 4ar - 24cf - 16cn + 16cr - 24ef + 112en - 112er + fh + 36fm + 36fq + 4hn + 8hr + 16mr - 16nq$$

$$B_4 = 0.25b^2gt + 4b^2n^2 - 4b^2nr + b^2pt + b^2r^2 + 4b^2tz + 0.5bcgs + 2bcps + 8besz + 4bfnp + 8bfrz + 2bgnr - 4f^2pz - 4gmps - 4gn^2p - 4gptz - 4gqsz - 4gr^2z - 4hpsz$$

$$B_5 = -2cgt - 8cn^2 + 8cnr - 8cpt - 8cr^2 - 8ctz - 2ct - egt - 4en^2 + 16enr - 4ept - 4er^2 - 4etz - et + gmt + 4gqt + hn^2 - 4hnr + 4hpt + 4hr^2 + htz + 0.25ht + 4mpt + 4mr^2 + 4mt + 4n^2q + 4qtz + qt$$

$$B_6 = -cgs - 4cps - 4csz - cs - 2egs - 8eps - 8esz - 2es + 0.5f^2g + 6f^2p + 6f^2z + 0.5f^2 + 2fgn + 2fgr - 2fn - 2fr + 2gms + 2gn^2 - 4gnr + 2gtz + 0.5gt + 2hsz + 0.5hs + 8mps + 8n^2p - 4nr + 8ptz + 2pt + 8qsz + 2qs + 8r^2z + 2r^2$$

$$B_7 = 12f^2p + 12f^2z + 2fgr - 8fnp - 2fn + 8frz - 4gnr + 8gpt + 8gqs + 8gr^2 + 8hps + 8ms + 8n^2 - 4nr + 8tz$$

$$B_8 = -4f^2mp - 4f^2qz - 2fgmr - 4fgnq - 4fhnp - 2fhrz + 4fmr + 2fnq + hnr$$

$$B_9 = cgsz + 0.25cgs + 4cpsz + cps - 8f^2pz - 4fgrz + 4fnp + 2gnr$$

$$C_1 = 16e^2gps + 16e^2sz - 32efgnp + 32efrz - 16f^2gmp - 16f^2gqz - 16f^2hpz - 16f^2mp$$
$$- 16f^2qz - 16gmpt - 16gmqs - 16gmr^2 - 16gn^2q - 16gqtz - 16hmps - 16hn^2p - 16hptz$$
$$- 16hqsz - 16hr^2z$$

$$C_2 = -2bct - bet + 0.25bht + 4bmt + bqt - c^2s - 2ces + 0.5cf^2 - 2cfn - 2cfr$$
$$+ 0.5cgt + 0.5chs - 4cnr + 2cpt + 2cqs + 2cr^2 - 2efn + 8ems + 8en^2 - 4enr$$
$$+ 8etz + 8fmr + 4fnq + 2hnr$$

$$C_3 = 0.25c^2gs + c^2ps + 4cfnp + 2cgnr + 4e^2sz + 8efrz - 4f^2mp - 4f^2qz - 4gmpt$$
$$- 4gmqs - 4gmr^2 - 4gn^2q - 4gqtz - 4hmps - 4hn^2p - 4hptz - 4hqsz - 4hr^2z$$

$$C_4 = 4bct + 16bet - 2bht - 8bmt - 8bqt + 8ces - 2cf^2 - 4cfn + 4cfr - cgt - chs$$
$$- 4cms - 4cn^2 - 4cpt - 4cqs - 4cr^2 - 4ctz - ct + 8e^2s - 8ef^2 - 2egt - 2ehs$$
$$- 8ems - 8en^2 + 16enr - 8ept - 8eqs - 8er^2 - 8etz - 2et + 0.5f^2h + 6f^2m + 6f^2q$$
$$+ 2fhn + 2fhr + 2gmt + 2hms + 2hn^2 - 4hnr + 2htz + 0.5ht + 8mpt + 8mqs$$
$$+ 8mr^2 + 8n^2q + 8qtz + 2qt$$

$$C_5 = -80b^2e^2t - 4b^2eht - 16b^2emt - 16b^2eqt + 4b^2hmt + 16b^2hqt + 16b^2mqt$$

$$C_6 = -16e^3s - 2e^2f^2 + 28e^2fn - 28e^2fr + 8e^2nr + 12ef^2m + 12ef^2q$$
$$+ 2efhr + 8efmr - 8efnq + 8egqt - 4ehnr + 8ehpt + 8ehqs$$
$$+ 8ehr^2 + 8emt - 8f^2mq - 4fhmr - 8fhnq$$

$$C_7 = -egs - 4eps - 4esz - es + 0.25f^2g + f^2p + f^2z + 0.25f^2 + fgn$$
$$+ 4fnp - 4frz - fr + gms + gn^2 + gtz + 0.25gt + hsz + 0.25hs + 4mps$$
$$+ 4n^2p + 4ptz + pt + 4qsz + qs + 4r^2z + r^2$$

$$C_8 = 4ef^2p + 4ef^2z + 2efgr - 8efnp - 2efn + 8efrz - 4egnr - 4enr$$
$$- 8f^2mp - 8f^2qz - 4fgmr - 4fhrz + 4fnq + 2hnr$$

$$C_9 = ef^2p + ef^2z + egpt + egqs + egr^2 + ehps + ems + en^2 + etz - 2fgnq$$
$$- 2fhnp + 2fmr$$

$$D_1 = -16f^2gmq - 16f^2hmp - 16f^2hqz - 16f^2mq - 16gmqt - 16hmpt - 16hmqs - 16hmr^2 - 16hn^2q - 16hqtz$$

$$D_2 = -bc^2t - 2bcet + 0.5bcht + 2bcqt + 8bemt - c^2es + 0.25c^2f^2 - c^2fr + 0.25c^2gt + 0.25c^2hs + c^2pt + c^2qs + c^2r^2 - 2cefn - 4cenr + 4cfnq + 2chnr + 4e^2ms + 4e^2n^2 + 4e^2tz + 8efmr - 4f^2mq - 4gmqt - 4hmpt - 4hmqs - 4hmr^2 - 4hn^2q - 4hqtz$$

$$D_3 = 8c^2et - c^2ht - 4c^2mt - 4c^2qt + 8ce^2t - 2ceht - 8cemt - 8ceqt + 2chmt + 8cmqt - 16e^3t + 8ehqt$$

$$D_4 = 4e^2s - 2ef^2 - 4efn + 4efr - egt - ehs - 4ems - 4en^2 - 4ept - 4eqs - 4er^2 - 4etz - et + 0.25f^2h + f^2m + f^2q + fhn - 4fmr + 4fnq + gmt + hms + hn^2 + htz + 0.25ht + 4mpt + 4mqs + 4mr^2 + 4n^2q + 4qtz + qt$$

$$D_5 = -2e^2f^2 + 4e^2fn - 4e^2fr + 8e^2nr + 4ef^2m + 4ef^2q + 2efhr + 8efmr - 8efnq - 4ehnr - 8f^2mq - 4fhmr$$

$$D_6 = -16e^4s + 32e^3fn - 32e^3fr + 16e^2f^2m + 16e^2f^2q + 16e^2gqt + 16e^2hpt + 16e^2hqs + 16e^2hr^2 + 16e^2mt - 32efhnq - 16f^2hmq - 16hmqt$$

$$D_7 = -4ac^2e + ac^2h + 4ac^2q + 16ae^2m - 16ahmq + 16c^2e^2 - 4c^2eh - 16c^2em - 16c^2eq + 4c^2hm + 16c^2mq - 16e^4 + 16e^2hq$$

Appendix III : Application of Cramer's rule for the determination of constants of Eqs. (39)

$$P_j = \frac{\begin{vmatrix} fr_j & (br_j^2 + c) & (br_j^2 + e) & -\frac{1}{2}(br_j^2 + c) \\ -fr_j & (gr_j^2 + h) & \frac{1}{2}(br_j^2 + c) & -(br_j^2 + e) \\ -nr_j & \frac{1}{2}(br_j^2 + c) & (zr_j^2 + m) & -\frac{1}{4}(br_j^2 + c) \\ rr_j & -(br_j^2 + e) & -\frac{1}{4}(br_j^2 + c) & (pr_j^2 + q) \end{vmatrix}}{\begin{vmatrix} (r_j^2 + a) & (br_j^2 + c) & (br_j^2 + e) & -\frac{1}{2}(br_j^2 + c) \\ (br_j^2 + c) & (gr_j^2 + h) & \frac{1}{2}(br_j^2 + c) & -(br_j^2 + e) \\ (br_j^2 + e) & \frac{1}{2}(br_j^2 + c) & (zr_j^2 + m) & -\frac{1}{4}(br_j^2 + c) \\ -\frac{1}{2}(br_j^2 + c) & -(br_j^2 + e) & -\frac{1}{4}(br_j^2 + c) & (pr_j^2 + q) \end{vmatrix}} T_j = \alpha_j T_j$$

$$Q_j = \frac{\begin{vmatrix} (r_j^2 + a) & fr_j & (br_j^2 + e) & -\frac{1}{2}(br_j^2 + c) \\ (br_j^2 + c) & -fr_j & \frac{1}{2}(br_j^2 + c) & -(br_j^2 + e) \\ (br_j^2 + e) & -nr_j & (zr_j^2 + m) & -\frac{1}{4}(br_j^2 + c) \\ -\frac{1}{2}(br_j^2 + c) & rr_j & -\frac{1}{4}(br_j^2 + c) & (pr_j^2 + q) \end{vmatrix}}{\begin{vmatrix} (r_j^2 + a) & (br_j^2 + c) & (br_j^2 + e) & -\frac{1}{2}(br_j^2 + c) \\ (br_j^2 + c) & (gr_j^2 + h) & \frac{1}{2}(br_j^2 + c) & -(br_j^2 + e) \\ (br_j^2 + e) & \frac{1}{2}(br_j^2 + c) & (zr_j^2 + m) & -\frac{1}{4}(br_j^2 + c) \\ -\frac{1}{2}(br_j^2 + c) & -(br_j^2 + e) & -\frac{1}{4}(br_j^2 + c) & (pr_j^2 + q) \end{vmatrix}} T_j = \beta_j T_j$$

$$R_j = \frac{\begin{vmatrix} (r_j^2 + a) & (br_j^2 + c) & fr_j & -\frac{1}{2}(br_j^2 + c) \\ (br_j^2 + c) & (gr_j^2 + h) & -fr_j & -(br_j^2 + e) \\ (br_j^2 + e) & \frac{1}{2}(br_j^2 + c) & -nr_j & -\frac{1}{4}(br_j^2 + c) \\ -\frac{1}{2}(br_j^2 + c) & -(br_j^2 + e) & rr_j & (pr_j^2 + q) \end{vmatrix}}{\begin{vmatrix} (r_j^2 + a) & (br_j^2 + c) & h_1(br_j^2 + e) & -\frac{1}{2}(br_j^2 + c) \\ (br_j^2 + c) & (gr_j^2 + h) & \frac{h_1}{2}(br_j^2 + c) & -(br_j^2 + e) \\ (br_j^2 + e) & \frac{1}{2}(br_j^2 + c) & h_1(zr_j^2 + m) & -\frac{1}{4}(br_j^2 + c) \\ -\frac{1}{2}(br_j^2 + c) & -(br_j^2 + e) & -\frac{h_1}{4}(br_j^2 + c) & (pr_j^2 + q) \end{vmatrix}} T_j = \gamma_j T_j$$

$$S_j = \frac{\begin{vmatrix} (r_j^2 + a) & (br_j^2 + c) & (br_j^2 + e) & fr_j \\ (br_j^2 + c) & (gr_j^2 + h) & \frac{1}{2}(br_j^2 + c) & -fr_j \\ (br_j^2 + e) & \frac{1}{2}(br_j^2 + c) & (zr_j^2 + m) & -nr_j \\ -\frac{1}{2}(br_j^2 + c) & -(br_j^2 + e) & -\frac{1}{4}(br_j^2 + c) & rr_j \end{vmatrix}}{\begin{vmatrix} (r_j^2 + a) & (br_j^2 + c) & (br_j^2 + e) & -\frac{h_3}{2}(br_j^2 + c) \\ (br_j^2 + c) & (gr_j^2 + h) & \frac{1}{2}(br_j^2 + c) & -h_3(br_j^2 + e) \\ (br_j^2 + e) & \frac{1}{2}(br_j^2 + c) & (zr_j^2 + m) & -\frac{h_3}{4}(br_j^2 + c) \\ -\frac{1}{2}(br_j^2 + c) & -(br_j^2 + e) & -\frac{1}{4}(br_j^2 + c) & h_3(pr_j^2 + q) \end{vmatrix}} T_j = \eta_j T_j$$

References

Banerjee, J. R., 2003. Free vibration of sandwich beams using the dynamic stiffness method. Computers and Structures 81(18), 1915-1922.

Banerjee, J. R., Sobey, A.J., 2005. Dynamic stiffness formulation and free vibration analysis of a three-layered sandwich beam. International Journal of Solids and Structures 42(8), 2181-2197.

Birman, V., 2002. On the Choice of Shear Correction Factor in Sandwich Structures. Journal of Sandwich Structures and Materials 4(1), 83-95.

Bozhevolnaya, E., Sun, J. Q., 2004. Free vibration analysis of curved sandwich beams. Journal of Sandwich Structures and Materials 6(1), 47-73

Choi, N. S., 2003. A double cantilever sandwich beam method for evaluating dynamic characteristics of rubber materials. JSME International Journal series C- Mechanical Systems Machine Elements & Manufacturing 46(2), 666-674.

Ganesan, N., Pradeep, V., 2005. Buckling and vibration of sandwich beams with viscoelastic core under thermal environments. Journal of Sound and Vibration 286(4-5), 1067-1074.

Hao, M., Rao, M.D., 2005. Vibration and damping analysis of a sandwich beam containing a viscoelastic constraining layer. Journal of Composite Materials 39(18), 1621-1643.

Howson, W.P., Zare, A., 2005. Exact dynamic stiffness matrix for flexural vibration of three-layered sandwich beams. Journal of Sound and Vibration 282(3-5), 753-767.

Icardi, U., 2001. A three-dimensional zig-zag theory for analysis of thick laminated beams. Composite Structures 52 (1), 123-135.

Icardi U., 2003. Applications of zig-zag theories to sandwich beams. Mechanics of Advanced Materials and Structures 10(1), 77-97.

Kapuria, S., Dumir, P. C., Jain, N. K., 2004. Assessment of zigzag theory for static loading, buckling, free and forced response of composite and sandwich beams. Composite Structures 64(3-4), 317-327.

Meyer-Piening, H. R., 2004. Application of the elasticity solution to linear sandwich beam, plate and shell analyses. Journal of Sandwich Structures and Materials 6(4), 295-312.

Nabarrete, A., de Almeida, S. F. M., and Hansen, J. S., 2003. Sandwich-plate vibration analysis: three-layer quasi-three-dimensional finite element model. AIAA Journal 41(8), 1547-1555.

Numayr, K. S., Qablan, H. A., 2005. Effect of torsion and warping on the free vibration of sandwich beams. Mechanics of Composite Materials 41(2), 109-118.

Plagianakos, T. S., Saravanos, D. A., 2004. High-order layerwise mechanics and finite element for the damped dynamic characteristics of sandwich composite beams. International Journal of Solids and Structures 41(24-25), 6853-6871.

Raville, M.E., Ueng, E., Lei, M., 1961. Natural frequencies of vibration of fixed-fixed sandwich beams. Journal of Applied Mechanics 28, 367-371.

Ruzzene, M., 2004. Vibration and sound radiation of sandwich beams with honeycomb truss core. Journal of Sound and Vibration 227(4-5), 741-763.

Sisemore, C.L., Darvennes, C.M., 2002. Transverse vibration of elastic-viscoelastic-elastic sandwich beams: compression–experimental and analytical study. Journal of Sound and Vibration 252(1), 155-167.

Sokolinsky, V. S., Nutt, S. R., Frostig, Y., 2002. Boundary condition effects in free vibrations of higher-order soft sandwich beams. AIAA Journal 40(6), 1220-1227.

Sokolinsky, V. S., Von Bremen, H. F., Lavoie, J. A., Nutt, S. R., 2004. Analytical and experimental study of free vibration response of soft-core sandwich beams. Journal of Sandwich Structures and Materials 6(3), 239-261.

Yang, M., Qiao, P., 2005. Higher-order impact modeling of sandwich structures with flexible core. International Journal of Solids and Structures 42(20), 5460-5490.

Yang, W. P., Chen, L. W., Wang, C. C., 2005. Vibration and dynamic stability of a traveling sandwich beam. Journal of Sound and Vibration 285(3), 597-614.

Wittrick, W. H., Williams, F. W., 1971. A general algorithm for computing natural frequencies of elastic structures. Quarterly Journal of Mechanics and Applied Mathematics 24(1), 263-284.